

1 **The complete mitochondrial genome of *Calyptogena***
2 ***marissinica* (Heterodonta: Veneroida: Vesicomidae):**
3 **insight into the deep-sea adaptive evolution of vesicomids**

4 **Mei Yang^{1,2,3,4}, Lin Gong^{1,2,3,4}, Jixing Sui^{1,2,3,4}, Xinzheng Li^{1,2,3,4*}**

5 1 Department of Marine Organism Taxonomy and Phylogeny, Institute of Oceanology, Chinese Academy of Sciences, 7 Nanhai
6 Road, Qingdao 266071, China, 2 Center for Ocean Mega-Science, Chinese Academy of Sciences, 7 Nanhai Road, Qingdao
7 266071, China, 3 Laboratory for Marine Biology and Biotechnology, Qingdao National Laboratory for Marine Science and
8 Technology, 1 Wenhai Road, Qingdao 266237, China, 4 University of Chinese Academy of Sciences, 19 Yuquan Road, Beijing
9 100049, China

10 * lixzh@qdio.ac.cn

11 **Abstract**

12 The deep sea is one of the most extreme environments on earth, with low oxygen, high hydrostatic
13 pressure and high levels of toxins. Species of the family Vesicomidae are among the dominant
14 chemosymbiotic bivalves found in this harsh habitat. Mitochondria play a vital role in oxygen usage
15 and energy metabolism; thus, they may be under selection during the adaptive evolution of deep-sea
16 vesicomids. In this study, the mitochondrial genome (mitogenome) of the vesicomid bivalve
17 *Calyptogena marissinica* was sequenced with Illumina sequencing. The mitogenome of *C. marissinica*
18 is 17,374 bp in length and contains 13 protein-coding genes, 2 ribosomal RNA genes (*rrnS* and *rrnL*)
19 and 22 transfer RNA genes. All of these genes are encoded on the heavy strand. Some special elements,
20 such as tandem repeat sequences, “G(A)_nT” motifs and AT-rich sequences, were observed in the
21 control region of the *C. marissinica* mitogenome, which is involved in the regulation of replication and
22 transcription of the mitogenome and may be helpful in adjusting the mitochondrial energy metabolism
23 of organisms to adapt to the deep-sea environment. The gene arrangement of protein-coding genes was
24 identical to that of other sequenced vesicomids. Phylogenetic analyses clustered *C. marissinica* with
25 previously reported vesicomid bivalves with high support values. Positive selection analysis revealed
26 evidence of adaptive change in the mitogenome of Vesicomidae. Ten potentially important adaptive
27 residues were identified, which were located in *cox1*, *cox3*, *cob*, *nad2*, *nad4* and *nad5*. Overall, this
28 study sheds light on the mitogenomic adaptation of vesicomid bivalves that inhabit the deep-sea
29 environment.

30 Introduction

31 Mitochondria, which descended from proteobacteria via endosymbiosis, are important organelles in
32 eukaryotic cells and are involved in various processes, such as ATP generation, signaling, cell
33 differentiation, growth and apoptosis [1]. Moreover, mitochondria have their own genetic information
34 system. In general, the metazoan mitogenome is a closed, circular DNA molecule, ranging from 12 to
35 20 kb in length and usually containing 37 genes: 13 protein-coding genes (PCGs) (*atp6*, *atp8*, *cox1-3*,
36 *cytb*, *nad1-6* and *nad4l*) of the respiratory chain, 2 ribosomal RNA (rRNA) genes (*rrnS* and *rrnL*) and
37 22 transfer RNA (tRNA) genes [2]. In addition, there are several noncoding regions in the mitogenome,
38 and the longest noncoding “AT-rich” region is known as the control region (CR), which includes
39 elements controlling the initiation and regulation of transcription and replication [3]. Owing to maternal
40 inheritance, variable gene order, a low frequency of gene recombination and different genes having
41 different evolutionary rates, mitochondrial sequences are widely used for species identification, genetic
42 diversity assessment and phylogenetics at various taxonomic levels [4–7].

43 Since the discovery of cold seeps and hydrothermal vents in the deep sea, the unique biological
44 communities that depend on chemosynthetic primary production have attracted the attention of
45 researchers [8–11]. These deep-sea environments lack sunlight and exhibit high pressure, low oxygen
46 and high levels of chemical toxicity due to various heavy metals, and the organisms that live there
47 show a series of adaptations compared with marine species in coastal environments [12–15].
48 Mitochondria are the energy metabolism centers of eukaryotic cells, which can generate more than 95%
49 of cellular energy through oxidative phosphorylation (OXPHOS) [3]. Therefore, mitochondrial PCGs
50 may undergo evolutionary selection in response to metabolic requirements in extremely harsh
51 environments. Numerous studies have found clear and compelling evidence of adaptive evolution in the
52 mitogenome of organisms from extreme habitats, including Tibetan humans [16], Chinese snub-nosed
53 monkeys [17], Tibetan horses [18–19], Tibetan wild yaks [20], galliform birds [21], and Tibetan
54 loaches [22].

55 The family Vesicomidae (Dall & Simpson, 1901) is widely distributed worldwide from shelf to
56 hadal depths and comprises specialized bivalves occurring in reducing environments such as
57 hydrothermal vents located in mid-ocean ridges and back-arc basins, cold seeps at continental margins
58 and whale falls [23–26]. Studies have shown that vesicomid bivalves rely upon the symbiotic
59 chemoautotrophic bacteria in their gills for all or part of nutrition [27–28]. Based on the shells and soft

60 body, the Vesicomidae is divided into two subfamilies: Vesicominae and Pliocardiinae. The
61 Vesicominae includes only one genus, *Vesicomya*, while Pliocardiinae currently contains 20 genera.
62 Among the 20 genera, *Calyptogena* is the most diverse group of deep-sea vesicomid bivalves in the
63 western Pacific region and its marginal seas [29]. As some of the dominant species in the deep sea,
64 vesicomids are an interesting taxon with which to study the mechanisms of adaptation to diverse
65 stressors in deep-sea habitats. Considering that the mitogenome has highly compact DNA and is easily
66 accessible, several complete/nearly complete mitogenomes of vesicomids have been sequenced [30–
67 33] in recent years; however, limited information is available about the mechanism of adaptation to
68 deep-sea habitats in vesicomids at the mitogenome level.

69 In the present study, we obtained the mitogenome of *Calyptogena marissinica*, a new species of the
70 family Vesicomidae from the Haima cold seep of the South China Sea. First, the mitogenome
71 organization, codon usage, and gene order information were obtained, and we compared the
72 composition of this mitogenome with that of other available vesicomid bivalve mitogenomes. Second,
73 based on mitochondrial PCGs and 2 rRNA genes, the phylogenetic relationships between *C.*
74 *marissinica* and other species from subclass Heterodonta were examined. Finally, to understand the
75 adaptive evolution of deep-sea organisms, we conducted positive selection analysis of vesicomid
76 bivalve mitochondrial PCGs.

77 **Materials and Methods**

78 **Sampling, identification and DNA extraction**

79 Specimens of *C. marissinica* were sampled from the “Haima” methane seep in the northern sector of
80 the South China Sea at a depth of 1,380–1,390 m using a remotely operated vehicle (ROV) in May
81 2018. Species-level morphological identification was performed according to the main points of Chen
82 et al. (2018) [29]. Specimens were preserved at -80°C until DNA extraction. Total genomic DNA was
83 extracted using a DNeasy tissue kit (Qiagen, Beijing, China) following the manufacturer's protocols.

84 **Illumina sequencing, mitogenome assembly and annotation**

85 After DNA isolation, 1 µg of purified DNA was fragmented, used to construct short-insert libraries
86 (insert size of 430 bp) according to the manufacturer's instructions (Illumina), and then sequenced on
87 an Illumina HiSeq 4000 instrument (San Diego, USA).

88 Prior to assembly, raw reads were filtered. This filtering step was performed to remove the reads

89 with adaptors, the reads showing a quality score below 20 ($Q < 20$), the reads containing a percentage of
90 uncalled bases (“N” characters) equal to or greater than 10% and the duplicated sequences. The
91 mitochondrial genome was reconstructed using a combination of *de novo* and reference-guided
92 assemblies, and the following three steps were used to assemble the mitogenome. First, the filtered
93 reads were assembled into contigs using SOAPdenovo 2.04 [34]. Second, contigs were aligned to the
94 reference mitogenomes from species of the family Vesicomidae using BLAST, and aligned contigs
95 ($\geq 80\%$ similarity and query coverage) were ordered according to the reference mitogenomes. Third,
96 clean reads were mapped to the assembled draft mitogenome to correct the incorrect bases, and the
97 majority of gaps were filled via local assembly.

98 The mitochondrial genes were annotated using homology alignments and *de novo* prediction, and
99 EVIDENCEModeler [35] was used to integrate the gene set. rRNA genes and tRNA genes were predicted
100 by rRNAMmer [36] and tRNAscan-SE [37]. A whole-mitochondrial genome BLAST search (E-value \leq
101 $1e^{-5}$, minimal alignment length percentage $\geq 40\%$) was performed against 5 databases, namely, the
102 KEGG (Kyoto Encyclopedia of Genes and Genomes), COG (Clusters of Orthologous Groups), NR
103 (Non-Redundant Protein), Swiss-Prot and GO (Gene Ontology) databases. Organellar Genome DRAW
104 [38] was used for circular display of the *C. marissinica* mitogenome.

105 **Sequence analysis**

106 The nucleotide composition and codon usage were computed using DnaSP 5.1 [39]. The AT and GC
107 skews were calculated with the following formulas: AT skew = $(A - T) / (A + T)$ and GC skew = $(G -$
108 $C) / (G + C)$ [40], where A, T, G and C are the occurrences of the four nucleotides. Tandem Repeats
109 Finder 4.0 [41] was used to search for the tandem repeat sequences. The online version of Mfold [42]
110 was applied to infer potential secondary structure, and if more than one secondary structure appeared,
111 the one with the lowest free energy score was used.

112 **Phylogenetic analysis**

113 The phylogeny of the subclass Heterodonta was reconstructed using mitogenome data from 41 species,
114 including 2 Lucinida species, 2 Myoida species, and 37 Veneroida species, and *Chlamys farreri* and
115 *Mimachlamys nobilis* from the subclass Pteriomorphia served as outgroups (S1 Table). Our data set
116 was based on nucleotide and amino acid sequences from 9 mitochondrial PCGs (*cox1*, *cox2*, *cox3*, *cob*,
117 *atp6*, *nad1*, *nad4*, *nad5*, and *nad6*) and 2 rRNA genes. The *atp8*, *nad2*, *nad4l* and *nad6* sequences were
118 excluded due to several species with incomplete mitogenomes. Multiple alignments of the 11 genes

119 were conducted using MUSCLE 3.8.31, followed by manual correction. In aligned sequences,
120 ambiguously aligned regions and gaps were removed using Gblocks server ver. 0.91b [43] with the
121 default setting. ModelTest 2.1.10 [44] and ProtTest 3.4 [45] were used to select the best-fit
122 evolutionary models GTR + I + G and LG + I + G + F for the nucleotide dataset and amino acid dataset,
123 respectively. Maximum likelihood (ML) analysis was performed using RAxML ver. 8.2.8 [46].
124 Topological robustness for the ML analysis was evaluated with 100 replicates of bootstrap support.
125 Bayesian inference (BI) was conducted using MrBayes 3.2.6 [47], and four Markov chain Monte Carlo
126 (MCMC) chains were run for 10^6 generations, with sampling every 100 generations and a 25% relative
127 burn-in. All phylogenetic trees were graphically edited with the iTOL 3.4.3
128 (<https://itol.embl.de/itol.cgi>).

129 **Positive selection analysis**

130 Comparing the nonsynonymous/synonymous substitution ratios ($\omega = dN/dS$) has become a useful
131 approach for quantifying the impact of natural selection on molecular evolution [48]. $\omega > 1$, $= 1$ and < 1
132 indicate positive selection, neutrality and purifying selection, respectively. The codon-based maximum
133 likelihood (CodeML) method implemented in the PAML package [49] was applied to estimate the
134 dN/dS ratio ω . The combined database of 13 mitochondrial PCGs was used for the selection pressure
135 analyses. Both the ML and Bayesian phylogenetic trees were separately used as the working topology
136 in all CodeML analyses.

137 To evaluate positive selection in the vesicomimid bivalves, we used branch models in the present
138 study. First, a one-ratio model (M_0), the simplest model, which allows only a single ω ratio for all
139 branches in the phylogeny [50], was used to preliminarily estimate the ω value for the gene sequences.
140 Then, a two-ratio model, which allows the background lineages and foreground lineages to have
141 different ω ratio values, was used to detect positive selection acting on branches of interest [51–52].
142 Last, a free-ratio model, which allows ω ratio variation among branches, was used to estimate ω values
143 on each branch [52]. Here, a one-ratio model and a free-ratio model were compared to confirm whether
144 different clades in Heterodonta had different ω values. Additionally, we compared a one-ratio model
145 and a two-ratio model to investigate whether deep-sea vesicomimid clades are subjected to more
146 selection pressure than other Heterodonta species in coastal waters. ω_0 and ω_1 represent the values for
147 the other Heterodonta clades in the phylogeny and the vesicomimid clades, respectively. Pairwise
148 models were compared with critical values of the Chi square (χ^2) distribution using likelihood ratio

149 tests (LRTs), in which the test statistic was estimated as twice the log likelihood ($2\Delta L$) and the degrees
150 of freedom were estimated as the difference in the number of parameters for each model.

151 Furthermore, we fit branch-site models to examine positive selection on some sites among the
152 vesicomid clades. Branch-site models allow ω to vary both among sites in the protein and across
153 branches on the tree. Branch-site model A (positive selection model) was used to identify the positively
154 selected sites among the lineages of vesicomids (marked as foreground lineages). The presence of
155 sites with $\omega > 1$ suggests that model A fits the data significantly better than the corresponding null
156 model. Bayes Empirical Bayes analysis was used to calculate posterior probabilities in order to identify
157 sites under positive selection on the foreground lineages if the LRTs was significant [53].

158 **Results and Discussion**

159 ***C. marissinica* mitogenome organization**

160 The Illumina HiSeq runs resulted in 20,359,890 paired-end reads from the *C. marissinica* library with
161 an insert size of approximately 450 bp. Selective-assembly analysis showed that 2,422 Mb of clean
162 data (Q20 quality score of 97.01%) was assembled into a 17,374-bp circular molecule, which
163 represented the complete mitogenome of *C. marissinica* (Fig 1 and Table 1). This length is shorter than
164 that of the complete mitogenome of other vesicomid bivalves, which ranges from 19,738 bp in
165 *Calyptogena magnifica* [30] to 19,424 bp in *Abyssogena phaseoliformis* [32]. The genome encodes 37
166 genes, including 13 PCGs, 2 rRNA genes, and 22 tRNA genes (duplication of *tRNA^{Leu}* and *tRNA^{Ser}*).
167 All of the genes are encoded on the heavy (H) strand, as consistently reported for other bivalves [32–
168 33,54], and transcribed in the same direction. A total of 2,287 bp of noncoding nucleotides are scattered
169 among 23 intergenic regions varying from 1 to 1,676 bp in length (Table 1). The largest noncoding
170 region (1,676 bp) is located between *tRNA^{Trp}* and *nad6* and is identified as the putative control region
171 (CR) due to its location and high A+T content (73.3%). Furthermore, there are four overlaps between
172 adjacent genes in the *C. marissinica* mitogenome with a size range of 1 to 5 bp (*tRNA^{Glu}* / *tRNA^{Ser(UCA)}*,
173 *tRNA^{Leu(UUA)}* / *nad1*, *rrnS* / *tRNA^{Met}*, and *cox3* / *tRNA^{Phe}*).

174 **Fig 1. Complete mitogenome map of *C. marissinica*.** All 37 genes are encoded on the heavy (H) strand. Genes for proteins and
175 rRNAs are shown with standard abbreviations. Genes for tRNAs are displayed by a single letter for the corresponding amino acid,
176 with two leucine tRNAs and two serine tRNAs differentiated by numerals.

177 **Table 1. Mitogenome organization of *C. marissinica*.**

Name	Strand	Range	Size		Codon			Intergenic nucleotides
			Nucleotides	Amino acids	Start	Stop	Anticodon	
<i>cox1</i>	+	1-1833	1833	610	ATG	TAA		-
<i>tRNA-Pro</i>	+	1854-1917	64				TGG	20
<i>cox2</i>	+	1918-2934	1017	338	ATG	TAA		0
<i>tRNA-Arg</i>	+	2941-3005	65				TCG	6
<i>cob</i>	+	3010-4143	1134	377	ATG	TAA		4
<i>rrnL</i>	+	4305-5340	1036					161
<i>atp8</i>	+	5377-5493	117	38	---	TAG		36
<i>nad4</i>	+	5506-6852	1347	448	ATG	TAA		12
<i>tRNA-His</i>	+	6873-6933	61				GTG	20
<i>tRNA-Glu</i>	+	6934-6999	66				TTC	0
<i>tRNA-Ser^{UCA}</i>	+	6996-7059	64				TGA	-4
<i>atp6</i>	+	7060-7773	714	237	ATG	TAA		0
<i>nad3</i>	+	7872-8192	321	106	ATT	TAA		98
<i>tRNA-Gln</i>	+	8203-8269	67				TTG	10
<i>tRNA-Ile</i>	+	8272-8338	67				GAT	2
<i>tRNA-Lys</i>	+	8339-8405	67				TTT	0
<i>tRNA-Leu^{UUA}</i>	+	8407-8469	63				TAA	1
<i>nad1</i>	+	8467-9381	915	304	ATA	TAG		-3
<i>tRNA-Val</i>	+	9399-9460	62				TAC	17
<i>tRNA-Asn</i>	+	9461-9522	62				GTT	0
<i>nad5</i>	+	9550-11223	1674	557	ATA	TAA		27
<i>tRNA-Leu^{CUA}</i>	+	11236-11297	62				TAG	12
<i>tRNA-Trp</i>	+	11298-11362	65				TCA	0
<i>contral region</i>	+	11363-13038	1676					0
<i>nad6</i>	+	13039-13554	516	171	ATT	TAA		0
<i>nad4l</i>	+	13595-13843	249	82	ATT	TAA		40
<i>tRNA-Gly</i>	+	13844-13907	64				TCC	0
<i>nad2</i>	+	13925-15010	1086	361	ATT	TAG		17
<i>tRNA-Asp</i>	+	15020-15081	62				GTC	9
<i>tRNA-Thr</i>	+	15082-15142	61				TGT	0
<i>rrnS</i>	+	15160-16027	868					17
<i>tRNA-Met</i>	+	16023-16089	67				CAT	-5
<i>tRNA-Cys</i>	+	16092-16153	62				GCA	2
<i>tRNA-Tyr</i>	+	16159-16220	62				GTA	5
<i>tRNA-Ser^{AGA}</i>	+	16228-16296	69				TCT	7
<i>cox3</i>	+	16297-17148	852	283	ATG	TAG		0
<i>tRNA-Phe</i>	+	17148-17210	63				GAA	-1
<i>tRNA-Ala</i>	+	17228-17293	66				TGC	17

178 The *C. marissinica* mitogenome has a nucleotide composition of 25.9% A, 10.8% C, 23.8% G, and
 179 39.5% T and an overall AT content of 65.4%. The AT skew and GC skew are well conserved among
 180 vesicomids, which vary from -0.165 to -0.230 and 0.343 to 0.440, respectively (Table 2). For the *C.*

181 *marissinica* mitogenome, the AT skew is -0.209, and the GC skew is 0.375, which indicates bias
182 toward T and G similar to that in other vesicomids. The complete mitochondrial DNA sequence has
183 been deposited in GenBank under accession number MK948426.

Table 2. Mitogenomes of Vesicomidae species sequenced to date and their genomic features.

Species	Genus	Accession number	Length (bp)	Genome			Protein-coding genes			rrnL	rrnS	tRNAs		Control region			
				AT%	AT skew	GC skew	Length (aa)	AT% (all)	AT% (3rd)	Length (bp)	AT%	Length (bp)	AT%	Number/Length(bp)	Length (bp)	AT%	
<i>Abyssogena mariana</i> ¹	<i>Abyssogena</i>	LC126311	15,927*	69.8	-0.210	0.408	3884	69.0	73.9	1196	71.2	862	70.8	23/1279	71.7	-	-
<i>Abyssogena phaseoliformis</i>	<i>Abyssogena</i>	AP014557	19,424	70.4	-0.199	0.440	3881	68.3	73.7	1196	71.2	862	70.9	24/1282	70.4	3438	74.4
<i>Akebiconcha kawamura</i> ²	<i>Akebiconcha</i>	AP014551	12,946*	65.2	-0.222	0.371	3249	62.5	68.7	1194	69.7	205	67.7	17/1090	69.0	-	-
<i>Archivesica gigas</i> ¹	<i>Archivesica</i>	MF959623	15,674*	65.0	-0.228	0.389	3878	63.6	70.6	1223	68.9	879	67.9	21/1212	68.7	-	-
<i>Archivesica pacifica</i> ¹	<i>Archivesica</i>	MF959624	17,782*	68.6	-0.214	0.429	4002	67.1	79.5	1226	71.3	885	69.9	22/1282	69.6	-	-
<i>Archivesica</i> sp. ¹	<i>Archivesica</i>	MF959622	15,650*	64.8	-0.228	0.386	3889	63.7	70.8	1221	69.0	879	67.8	20/1214	68.7	-	-
<i>Calyptogena fausta</i> ²	<i>Calyptogena</i>	AP014549	13,509*	66.0	-0.218	0.394	3410	64.7	70.7	1189	70.3	205	67.8	17/1092	70.0	-	-
<i>Calyptogena laubirei</i> ²	<i>Calyptogena</i>	AP014553	12,968*	64.3	-0.226	0.361	3259	61.6	67.1	1191	69.0	204	67.2	17/1090	67.8	-	-
<i>Calyptogena magnifica</i>	<i>Calyptogena</i>	NC_028724	19,738	68.4	-0.195	0.390	3928	65.5	75.6	1219	70.5	935	70.0	22/1347	70.2	3910	75.2
<i>Calyptogena marissinica</i>	<i>Calyptogena</i>		17,374	65.4	-0.209	0.375	3912	63.2	69.7	1,036	67.2	868	67.7	22/1,411	68.7	1676	73.3
<i>Calyptogena nautili</i> ²	<i>Calyptogena</i>	AP014554	13,281*	69.4	-0.196	0.353	3298	68.0	74.4	1182	72.1	204	72.1	17/1088	71.4	-	-
<i>Calyptogena pacifica</i> ²	<i>Calyptogena</i>	AP014556	13,454*	67.6	-0.222	0.420	3390	66.6	72.6	1195	70.8	204	69.6	17/1088	69.5	-	-
<i>Isorropodon fossajaponicum</i> ¹	<i>Isorropodon</i>	AP014550	19,556*	68.2	-0.165	0.343	3894	66.6	70.6	1199	70.3	861	68.3	24/1290	70.3	-	-
<i>Phreagena kilmeri</i> ²	<i>Phreagena</i>	AP014552	12,944*	64.9	-0.223	0.365	3249	63.4	68.0	1191	69.5	204	68.3	17/1089	68.7	-	-
<i>Phreagena okutani</i> ¹	<i>Phreagena</i>	AP014555	16,336*	65.6	-0.230	0.405	3833	64.0	68.1	1191	69.7	861	67.7	23/1277	68.9	-	-
<i>Phreagena soyoae</i> ²	<i>Phreagena</i>	AP014558	12,941*	64.9	-0.223	0.365	3249	63.4	67.9	1190	69.5	204	68.1	17/1089	68.7	-	-
<i>Pliocardia stearnsii</i> ²	<i>Pliocardia</i>	AP014559	13,012*	67.7	-0.230	0.402	3265	66.6	72.7	1201	71.6	203	69.5	17/1096	69.1	-	-

185

Note: * indicates incomplete mitogenomes.

186

¹ Incomplete mitogenomes for which the control region was not sequenced.

187

² Incomplete mitogenomes for which *nad2*, *nad4l*, *nad6*, a few tRNA genes and the control region were not sequenced.

188 **Protein-coding genes**

189 The total length of all 13 PCGs of *C. marissinica* is 11,775 bp, accounting for 67.8% of the complete
190 length of the mitogenome, and the PCGs encode 3,912 amino acids (Table 2). In the mitogenome of
191 metazoans, most PCGs start with the standard ATN codon [2,55–56]. In the present study, with the
192 exception of the *atp8* gene, which had the alternate initiation codon GTG, all the PCGs were initiated
193 by typical ATN codons: 6 genes (*atp6*, *cob*, *cox1*, *cox2*, *cox3*, and *nad4*) were initiated by ATG, 4
194 genes (*nad2*, *nad3*, *nad4l*, and *nad6*) were initiated by ATT, and 2 genes (*nad1* and *nad5*) were
195 initiated by ATA. Notably, genes are commonly initiated by GTG in vesicomid bivalves [31], and the
196 amino acid encoded by GTG is valine, which belongs to the nonpolar amino acids, such as methionine
197 and isoleucine encoded by ATN. Moreover, in eight other vesicomid bivalves (*Archivesica* sp.,
198 *Archivesica gigas*, *Archivesica pacifica*, *C. magnifica*, *Abyssogena mariana*, *Ab. phaseoliformis*,
199 *Isorropodon fossajaponicum*, and *Phreagena okutanii*), *cox3* had a truncated termination codon, TA
200 [31]. Previous studies have shown that the truncated stop codon is common in the metazoan
201 mitogenome and might be corrected by posttranscriptional polyadenylation [57–58]. However, in the
202 mitogenome of *C. marissinica*, all of the PCGs were ended by a complete TAA (*atp6*, *cob*, *cox1*, *cox2*,
203 *nad3*, *nad4*, *nad4l*, *nad5*, and *nad6*) or TAG (*atp8*, *cox3*, *nad1*, and *nad2*) termination codon.

204 Numerous studies have indicated that metazoan mitogenomes usually have a bias toward a higher
205 representation of nucleotides A and T, leading to a subsequent bias in the corresponding encoded
206 amino acids [56,59–61]. In the mitogenome of *C. marissinica*, the A+T contents of PCGs and third
207 codon positions are 63.2% and 69.7%, respectively, which are similar to the values observed in other
208 vesicomids (Table 2). The amino acid usage and relative synonymous codon usage (RSCU) values in
209 the PCGs of *C. marissinica* are summarized in Fig 2. The mitogenome encodes a total of 3,912 amino
210 acids, among which leucine (13.6%) and glutamine (1.4%) are the most and the least frequently used,
211 respectively. As mentioned earlier, the amino acids encoded by A+T-rich codon families (Asn, Ile, Lys,
212 Met, Phe and Tyr) have a higher frequency of use than those encoded by G+C-rich codon families (Ala,
213 Arg, Gly and Pro). The RSCU values indicate that the six most commonly used codons are TTA (Leu),
214 ACT (Thr), GGG (Gly), TCT (Ser), GCT (Ala), and CCT (Pro) (Fig 2), which show A+T bias at their
215 third codon position. In addition, the codons with A and T in the third position are used more
216 frequently than other synonymous codons. These features reflect codon usage with A and T biases at
217 the third codon position, which are similar to the biases that exist in many metazoans [62–65].

218 **Fig 2. Codon usage (A) and the relative synonymous codon usage (RSCU) (B) of the *C. marissinica* mitogenome.** Numbers
219 to the left refer to the total number of codons (A) and the RSCU values (B). Codon families are provided on the X axis.

220 **Ribosomal RNA and transfer RNA genes**

221 The *rrnL* and *rrnS* genes of *C. marissinica* are 1,036 bp (AT% = 67.2) and 868 bp (AT% = 67.7) in
222 length, respectively. As in other vesicomid bivalves, *rrnL* is located between the *cytb* and *atp8* genes,
223 and *rrnS* is located between *tRNA^{Thr}* and *tRNA^{Met}*. The largest known *rrnL* and *rrnS* genes are 1,226 bp
224 in *Ar. pacific* and 935 bp in *C. magnifica*, respectively [30–32].

225 Twenty-two tRNA genes were identified in the mitogenome of *C. marissinica*, which is typical for
226 metazoans. However, the number of tRNA genes varies among other vesicomid bivalves (Table 2).
227 The length of tRNA genes in *C. marissinica* ranges from 61 (*tRNA^{His}* and *tRNA^{Thr}*) to 69 (*tRNA^{Ser(AGA)}*)
228 bp (Table 1), and the AT content of the tRNA genes is 68.7%. The secondary structures of tRNA genes
229 are schematized in S1 Fig. Generally, a typical tRNA clover-leaf structure includes a 7-8 bp aminoacyl
230 acceptor stem, a 3-5 bp T Ψ C stem, a 5 bp anticodon stem and a 4 bp DHU stem. In the present study,
231 most of the tRNA genes had the typical secondary structure, except for *tRNA^{His}*, *tRNA^{Thr}*, *tRNA^{Tyr}*,
232 *tRNA^{Ser(UCA)}* and *tRNA^{Ser(AGA)}*. In *tRNA^{His}*, *tRNA^{Thr}* and *tRNA^{Tyr}*, the T Ψ C loops are incomplete, which is
233 not observed in other vesicomid bivalves [31–33], and this feature might be a specific character in the
234 *C. marissinica* mitogenome. In *tRNA^{Ser(UCA)}* and *tRNA^{Ser(AGA)}*, the DHU stems are reduced to a simple
235 loop, as in many other bivalve mitogenomes [31,66]. Many studies have shown that the incomplete
236 clover-leaf secondary structure of tRNA genes is common in metazoan mitogenomes and that aberrant
237 tRNA genes can still function normally through posttranscriptional RNA editing and/or coevolved
238 interacting factors [67–69]. Additionally, several mismatch pairs were detected within amino acid
239 acceptors and anticodon stems in tRNA genes of *C. marissinica*. Such mismatches seem to be
240 ubiquitous phenomena in the mitogenomes of many organisms and can also be corrected by
241 posttranscriptional RNA editing [56,64,70–71].

242 **Noncoding regions and gene arrangement**

243 A total of 23 noncoding regions (totaling 2,216 bp) are distributed in the *C. marissinica* mitogenome.
244 The longest noncoding region (1,676 bp), located between *tRNA^{Trp}* and *nad6*, corresponds to the
245 control region identified in most other vesicomids. The nucleotide content of the 1,676 bp control
246 region is 34.25% A, 39.02% T, 16.29% G, and 10.44% C. The A + T content (73.27%) of this region is
247 higher than that of other regions in the *C. marissinica* mitogenome (Table 2). In general, the

248 mitochondrial control region is subjected to less evolutionary pressure than PCGs and thus has the
249 highest variation in the whole mitogenome [72–73].

250 Additionally, in the mitochondrial control region of *C. marissinica*, we found a tandemly arranged
251 repeated sequence, which was 354 bp in length (positions 12,675–13,028), including three identical
252 tandem repeat units of 118 bp (Fig 3). The tandem repeat sequence could be folded into stem-loop
253 secondary structures with minimized free energy (Fig 3), which is a common phenomenon in
254 invertebrates [61,64–65,74]. The control region in the mitogenome is essential for transcription and
255 replication in animals [75–76]. Therefore, the stem-loop structures mentioned above may play an
256 important role in gene replication and regulation. In addition, some other peculiar patterns, such as
257 special “G(A)_nT” motifs and AT-rich sequences, were observed in the control region of the *C.*
258 *marissinica* mitogenome (Fig 3). Furthermore, similar characteristics (e.g., repetitive elements, G(A)_nT
259 motifs and AT-rich sequences) were also observed in the deep-sea anemone *Bolocera* sp., alvinocaridid
260 shrimp *Shinkaicaris leurokolos* and spongiolid shrimp *Spongiocaris panglao* [61,64–65]. In view of
261 the particularity of the deep-sea environment, we speculate that these special control region elements
262 are involved in the regulation of replication and transcription of the mitogenome and help organisms
263 adapt to extreme deep-sea habitats.

264 **Fig 3. Nucleotide sequences and stem-loop structures of the tandem repeat motifs in the control region (CR) of the *C.***
265 ***marissinica* mitogenome.** The CR is flanked by sequences encoding *tRNA^{Trp}* and *nad6*. The CR consists of certain patterns, such
266 as special G(A)_nT motifs (marked with a box), AT-rich regions and tandem repeat motifs.

267 In contrast to other metazoans, the Mollusca showed frequent and extensive variation in gene
268 arrangement, and among them, bivalves showed more gene order variation in their mitogenomes [77–
269 79]. Here, a comparison of the *C. marissinica* mitogenome with the other twelve Heterodonta
270 mitogenomes is shown in Fig 4. All thirteen Heterodonta mitogenomes come from two orders (five
271 families): Myoida (family Hiattellidae) and Veneroida (family Tellinidae, family Mactridae, family
272 Veneridae and family Vesicomomyidae). Among the Heterodonta mitogenomes analyzed in the present
273 study, the gene arrangement has a distinct difference between the family Vesicomomyidae and other
274 species (Fig 4). In the family Vesicomomyidae, we found that if the tRNA genes are not considered, the
275 nine vesicomomyid bivalves have a completely identical gene arrangement of PCGs. When compared to
276 the “standard” mitogenome of *Ar. pacific*, *C. magnifica* and *C. marissinica*, several additional tRNA
277 genes were identified in *Ab. mariana* (*tRNA^{Leu3}*), *Ab. phaseoliformis* (*tRNA^{His2}* and *tRNA^{Ser3}*), *I.*
278 *fossajaponicum* (*tRNA^{Asn2}* and *tRNA^{Lys2}*) and *Ph. okutanii* (*tRNA^{Met2}*) (Fig 4). As a general rule,

279 additional gene copies usually obtained by gene replication and different gene copies would share some
280 sequence identity with each other. However, analysis showed that the aforementioned additional tRNA
281 genes have low similarity to other tRNA genes that encode the same tRNAs [31]. The remodeling of
282 tRNA genes, DNA shuffling and the point mutations in the anticodons may all provide chances for
283 tRNA gene rearrangement within mitogenomes [3,80–81]. Furthermore, gene rearrangements usually
284 occurred around the control regions, which are considered the replication origins. Perhaps gene
285 replication events occur frequently in this region, and consequently, more novel gene arrangements will
286 be found in this region. To date, there are four known mechanisms of gene rearrangements in
287 mitogenomes: inversion, transposition, reverse transposition and tandem duplication-random losses
288 (TDRLs) [82–83]. However, the specific mechanism of significant differences in mitochondrial gene
289 arrangements in mollusks has not been completely clarified. With the determination of mitogenomes in
290 more species of this phylum, the mechanism of large-scale rearrangement of mitochondrial genes in
291 mollusks will be identified by further comparing and summarizing the rules of gene arrangement
292 among different species.

293 **Fig 4.** Mitochondrial gene arrangement of 13 species in the subclass Heterodonta (*Panopea generosa*, *Moerella iridescens*,
294 *Coelomactra antiquata*, *Meretrix meretrix* and 9 vesicomid clams). CR indicates the control region. Genes for tRNAs are
295 displayed by a single letter for the corresponding amino acid, with two leucine tRNAs and two serine tRNAs differentiated by
296 numerals. Uniquely derived gene positions of individual species are depicted in red. Sequence segments are not drawn to scale.

297 **Phylogenetic relationships**

298 Since several vesicomid bivalves have incomplete mitogenomes at present, phylogenetic analyses
299 were performed based on nucleotide and amino acid sequences of 9 mitochondrial PCGs (*atp6*, *cox1*,
300 *cox2*, *cox3*, *cob*, *nad1*, *nad3*, *nad4*, and *nad5*) and 2 rRNA genes by maximum likelihood (ML) and
301 Bayesian inference (BI) methods (Fig 5, S1-S3 Fig). The tree topologies resulting from the BI and ML
302 analyses were not the same. There are two potential reasons for this discrepancy: one is that the
303 presence of noncoding rRNA genes made the databases of nucleotides and amino acids different, and
304 the other is the fact that several clades are represented by only one or two species each. The
305 phylogenetic analyses clustered *C. marissinica* with the previously reported vesicomid bivalves with
306 high support values (Fig 5). In all phylogenetic trees, the family Vesicomidae first clustered well with
307 Veneridae and then united with Mactridae, which corroborates earlier studies of phylogenetic
308 relationships based on the concatenated 12 PCGs and 2 rRNA genes [31–33]. *Calypptogena (sensu lato)*
309 is the most diverse group of deep-sea vesicomid bivalves in the western Pacific region and its

310 marginal seas. Until now, the composition, evolutionary position and level of the genus *Calyptogena*
311 have been the subject of discussion [84–86]. Phylogenetic reconstruction using the cytochrome oxidase
312 *c* subunit I (*cox1*) gene showed that *C. marissinica* was clearly nested within a fully supported
313 monophyletic clade corresponding to *Calyptogena sensu lato* and consisting of all included
314 *Calyptogena (sensu lato)* species [29]. Notably, in our studies, *C. marissinica* showed a
315 close genetic relationship with the *Akebiconcha* species (Fig 5). Therefore, additional mitogenomes of
316 a greater number of vesicomylid bivalves, combined with morphological characters, are necessary to
317 determine the phylogenetic relationships among members of this family.

318 **Fig 5. Phylogenetic tree derived from Bayesian analyses based on concatenated nucleotide sequences of 9 mitochondrial**
319 **PCGs (*cox1*, *cox2*, *cox3*, *cob*, *atp6*, *nad1*, *nad4*, *nad5*, and *nad6*) and 2 ribosomal RNA genes (*rrnS* and *rrnL*).** Numbers on
320 branches are Bayesian posterior probabilities (percent). Two Pectinidae species belonging to the subclass Pteriomorpha were
321 used as outgroups.

322 **Positive selection analysis**

323 Purifying selection is the predominant force in the evolution of mitogenomes, but because
324 mitochondria are the main sites of aerobic respiration and are essential for energy metabolism, weak
325 and/or episodic positive selection may occur against this background of strong purifying selection
326 under reduced oxygen availability or greater energy requirements [87–88]. As proven by many studies,
327 mitochondrial PCGs underwent positive selection in animals that survived in hypoxic environments or
328 had higher energy demands for locomotion, such as Tibetan humans, Ordovician bivalves, diving
329 cetaceans and flying insects [16,89–91].

330 Considering that the special habitats of the deep sea may impact the function of mitochondrial genes,
331 we examined potential positive selection in the Vesicomylidae lineage using CodeML from the PAML
332 package. Although different tree-building methods were used, the results of positive selection analyses
333 were generally consistent (Table 3). In the analysis of branch models, the ω (dN/dS) ratio calculated
334 under the one-ratio model (M_0) was 0.02272 for the 13 mitochondrial PCGs of sampled Heterodonta
335 bivalves, suggesting that these genes have experienced constrained selection pressure to maintain
336 function. Then, in the comparison of the one-ratio model (M_0) and the free-ratio model, the LRTs
337 indicated that the free-ratio model fit the data better than the one-ratio model (Table 3), which means
338 that the ω ratios are indeed different among lineages. Furthermore, the two-ratio model was also found
339 to fit the data better than the one-ratio model (Table 3) when the family Vesicomylidae was set as a
340 foreground branch. The ω ratio of the Vesicomylidae branch was almost treble that of other branches

341 ($\omega_1 = 0.06398$ and $\omega_0 = 0.02278$), indicating divergence in selection pressure between vesicomylid
342 bivalves and other shallow-sea Heterodonta species. However, the ω ratio of the family Vesicomylidae
343 ($\omega_1 = 0.06398$) was still significantly less than 1. This result is consistent with the known functional
344 significance of mitochondria as a respiration chain necessary for electron transport and OXPHOS [92].

Table 3 CODEML analyses of selection pressure on mitochondrial genes in the Vesicomidae lineage.

Trees	Models	lnL	Parameter estimates	Models compared	2ΔL	p-value
Branch models						
Bayesian tree	M0	-203672.1001	$\omega = 0.02272$			
	Two-ratio	-203666.6298	$\omega_0 = 0.02278 \quad \omega_1 = 0.06398$	Two-ratio vs. M0	10.94072	0.00094
	Free-ratio	-202667.8186		Free-ratio vs. M0	2008.56299	0.00000
ML tree	M0	-203672.1001	$\omega = 0.02272$			
	Two-ratio	-203666.6298	$\omega_0 = 0.02278 \quad \omega_1 = 0.06398$	Two-ratio vs. M0	10.94072	0.00094
	Free-ratio	-202747.0065		Free-ratio vs. M0	1850.18729	0.00000
Branch-site models						
Bayesian tree	Null model	-202664.0952	$P_0 = 0.77667 \quad P_1 = 0.02562 \quad P_{2a} = 0.19139 \quad P_{2b} = 0.00631$ $\omega_0 = 0.02110 \quad \omega_1 = 1.00000 \quad \omega_{2a} = 1.00000 \quad \omega_{2b} = 1.00000$			
	Model A	-202663.7531	$P_0 = 0.78464 \quad P_1 = 0.02590 \quad P_{2a} = 0.18340 \quad P_{2b} = 0.00605$ $\omega_0 = 0.02115 \quad \omega_1 = 1.00000 \quad \omega_{2a} = 1.21998 \quad \omega_{2b} = 1.21998$	Model A vs. Null model	0.68422	0.40814
ML	Null model	-202664.0952	$P_0 = 0.77667 \quad P_1 = 0.02562 \quad P_{2a} = 0.19140 \quad P_{2b} = 0.00631$ $\omega_0 = 0.02110 \quad \omega_1 = 1.00000 \quad \omega_{2a} = 1.00000 \quad \omega_{2b} = 1.00000$			
	Model A	-202663.7531	$P_0 = 0.77667 \quad P_1 = 0.02562 \quad P_{2a} = 0.19139 \quad P_{2b} = 0.00631$ $\omega_0 = 0.02115 \quad \omega_1 = 1.00000 \quad \omega_{2a} = 1.22003 \quad \omega_{2b} = 1.22003$	Model A vs. Null model	0.68422	0.40814

347 Moreover, many studies have shown that positive selection often occurs over a short period of
 348 evolutionary time and acts on only a few sites; thus, the signal for positive selection is usually
 349 swamped by those for continuous purifying selection that occur on most sites in a gene sequence
 350 [87,93]. In the present study, branch-site models were used to detect possible positively selected sites in
 351 the vesicomylid bivalves (Table 4). Ten residues, which were located in *cox1*, *cox3*, *cob*, *nad2*, *nad4*
 352 and *nad5*, were identified as positively selected sites with high BEB values (> 95%).

353 **Table 4 Possible sites under positive selection in the Vesicomylidae lineage.**

Bayesian tree				ML tree			
Gene	Codon	Amino acid	BEB values	Gene	Codon	Amino acid	BEB values
<i>cox1</i>	529	W	0.967	<i>cox1</i>	529	W	0.967
<i>cox3</i>	998	G	0.956	<i>cox3</i>	998	G	0.956
	1018	W	0.962		1018	W	0.962
	1021	T	0.954		1021	T	0.954
<i>cob</i>	1131	K	0.982	<i>cob</i>	1131	K	0.982
	1432	A	0.959		1432	A	0.959
<i>nad2</i>	2043	K	0.960	<i>nad2</i>	2043	K	0.960
<i>nad4</i>	2388	E	0.951	<i>nad4</i>	2388	E	0.951
<i>nad5</i>	2734	P	0.975	<i>nad5</i>	2734	P	0.975
	2773	S	0.951		2773	S	0.951

354 It is well known that mitochondrial PCGs play a key role in the oxidative phosphorylation pathway;
 355 the above ten amino acid mutation sites are components of the respiratory chain and therefore may
 356 have important functions. As the first and the largest enzyme complex in the respiratory chain, the
 357 NADH dehydrogenase complex exercises the functions of proton pumps, and variation in loci may
 358 affect metabolic efficiency [90]. In this work, there were four positively selected sites located in the
 359 *nad2*, *nad4* and *nad5* genes. Similar results have been obtained in studies of the adaptive evolution of
 360 Tibetan horses, Chinese snub-nosed monkeys and Tibetan loaches, which live in high-altitude habitats
 361 [17,19,22]. Two residues in the *cob* gene were identified to be under positive selection. As a relatively
 362 conserved gene, *cob* plays a fundamental role in energy production in mitochondria. It catalyzes
 363 reversible electron transfer from ubiquinol to cytochrome *c* coupled to proton translocation [94]. Wide
 364 variation in the properties of amino acids was observed in functionally important regions of *cob* in
 365 species with more specialized metabolic requirements, such as adaptation to a low-energy diet or large
 366 body size and adaptation to unusual oxygen requirements or low-temperature environments [90,95].
 367 Cytochrome *c* oxidase, which catalyzes the terminal reduction of oxygen and whose catalytic core is
 368 encoded by three mitochondrial protein-coding genes (*cox1*, *cox2* and *cox3*), has been proven to be a
 369 particularly important target of positive selection during hypoxia adaptation [96–97]. Four positively
 370 selected residues were detected in the *cox1* and *cox3* genes. For *C. marissinica*, functional modification

371 mediated by positively selected mutations may increase the affinity between the enzyme and oxygen,
372 thus allowing the efficient utilization of oxygen under hypoxia and maintaining essential metabolic
373 levels.

374 The environment of deep-sea hydrothermal vents and cold seeps is characterized by darkness, a lack
375 of photosynthesis-derived nutrients, high hydrostatic pressure, variable temperatures, low dissolved
376 oxygen, and high concentrations of hydrogen sulfide (H₂S), methane (CH₄) and heavy metals, such as
377 iron, copper and zinc. Previous studies have confirmed that all of the above environmental factors
378 influence the process of mitochondrial aerobic respiration; for example, thirty potentially important
379 adaptive residues were identified in the mitogenome of *S. leurokolos* and revealed the mitochondrial
380 genetic basis of hydrothermal vent adaptation in alvinocaridid shrimp [65]. Similar findings have been
381 reported in other deep-sea macrobenthos, such as the sea anemone *Bolocera* sp., starfish *Freyastera*
382 *benthophila* and sea cucumber *Benthoctes marianensis* [64,98–99]. In the present study, ten
383 potentially adaptive residues were identified in the *cox1*, *cox3*, *cob*, *nad2*, *nad4* and *nad5* genes,
384 supporting the adaptive evolution of the mitogenome of *C. marissinica*. Our results at least
385 partly explained how the deep-sea vesicomid bivalves maintain aerobic respiration for sufficient
386 energy in the extremely harsh deep-sea environment. The findings of this study could help deepen our
387 understanding of the molecular mechanisms of adaptive evolution at the mitochondrial level in deep-
388 sea organisms.

389 **Conclusion**

390 This study characterized the complete mitogenome of the deep-sea vesicomid bivalve *C. marissinica*,
391 which is 17,374 bp in length and encodes 37 typical mitochondrial genes, including 13 PCGs, 2 rRNA
392 genes, and 22 tRNA genes. All of these genes are encoded on the heavy strand. We analyzed the
393 mitogenome organization, codon usage, control region features, gene arrangement, phylogenetic
394 relationships and positive selection of *C. marissinica*. In the mitogenome of *C. marissinica*, tandem
395 repeat sequences, “G(A)_nT” motifs and AT-rich sequences were detected. In the family Vesicomidae,
396 we found that if the tRNA genes are not considered, the sequenced vesicomid bivalves have a
397 completely identical arrangement of PCGs. The phylogenetic analyses clustered *C. marissinica* with
398 previously reported vesicomid bivalves with high support values. Ten residues located in *cox1*, *cox3*,
399 *cob*, *nad2*, *nad4* and *nad5* were inferred to be positively selected sites along the branches leading to
400 vesicomid bivalves, which may indicate that the genes were under positive selection pressure. This

401 study probes the mitochondrial genetic basis of deep-sea adaptation in vesicomyids and provides
402 valuable insight into the adaptation of organisms to the extreme deep-sea environment.

403 **Supporting information**

404 **S1 Table. Species used for phylogenetic reconstructions.**

405 **S2 Table. Species used for CodeML analyses of selective pressure on mitochondrial genes.**

406 **S1 Fig. Putative secondary structures for the 22 transfer RNAs of the *C. marissinica* mitogenome.**

407 **S2 Fig. Phylogenetic trees derived from ML analyses based on nucleotide sequences of 9
408 mitochondrial protein-coding genes and 2 ribosomal RNA genes.**

409 **S3 Fig. Phylogenetic trees derived from Bayesian analyses based on amino acid sequences of 9
410 mitochondrial protein-coding genes and 2 ribosomal RNA genes.**

411 **S4 Fig. Phylogenetic trees derived from ML analyses based on amino acid sequences of 9
412 mitochondrial protein-coding genes and 2 ribosomal RNA genes.**

413 **Acknowledgments**

414 The authors thank the captains and crews of the R/V Tan Suo Yi Hao and the pilots of
415 the HOV “Shen Hai Yong Shi” for technical support. This research is funded by the National Key
416 R&D Program of China (2018YFC0309804), the National Natural Science Foundation of China (NO.
417 41506173) and the Strategic Priority Research Program of the Chinese Academy of Sciences (No.
418 XDB06010101).

419 **References**

- 420 1. Martijn J, Vosseberg J, Guy L, Offre P, Ettema TJG. Deep mitochondrial origin outside the
421 sampled alphaproteobacteria. *Nature*. 2018; 557: 101–105. [https://doi.org/10.1038/s41586-018-](https://doi.org/10.1038/s41586-018-0059-5)
422 [0059-5](https://doi.org/10.1038/s41586-018-0059-5) PMID: [29695865](https://pubmed.ncbi.nlm.nih.gov/29695865/)
- 423 2. Wolstenholme DR. Animal mitochondrial DNA: Structure and evolution. *International Review of*
424 *Cytology*. 1992; 141: 173–216. PMID: [1452431](https://pubmed.ncbi.nlm.nih.gov/1452431/)
- 425 3. Boore JL. Animal mitochondrial genomes. *Nucleic Acids Research*. 1999; 27: 1767–1780. PMID:
426 [10101183](https://pubmed.ncbi.nlm.nih.gov/10101183/)
- 427 4. Hebert P, Cywinska A, Ball S, Waard J. Biological identification through DNA barcodes.
428 *Proceedings of the Royal Society B Biological Sciences*. 2002; 270: 313–321. [https://doi.org/10.10](https://doi.org/10.1098/rspb.2002.2218)
429 [98/rspb.2002.2218](https://doi.org/10.1098/rspb.2002.2218) PMID: [12614582](https://pubmed.ncbi.nlm.nih.gov/12614582/)

- 430 5. Gissi C, Iannelli F, Pesole G. Evolution of the mitochondrial genome of Metazoa as exemplified by
431 comparison of congeneric species. *Heredity*. 2008; 101: 301–320. [http://doi.org/10.1038/hdy.2008.](http://doi.org/10.1038/hdy.2008.62)
432 [62](#) PMID: [18612321](#)
- 433 6. Tan MH, Gan HM, Lee YP, Linton S, Grandjean F, Bartholomei-Santos ML, et al. ORDER within
434 the chaos: Insights into phylogenetic relationships within the Anomura (Crustacea: Decapoda)
435 from mitochondrial sequences and gene order rearrangements. *Molecular Phylogenetics and*
436 *Evolution*. 2018; 127: 320–331. <https://doi.org/10.1016/j.ympev.2018.05.015> PMID:
437 [29800651](#)
- 438 7. Schuster A, Vargas S, Knapp IS, Pomponi SA, Toonen RJ, Erpenbeck D, et al. Divergence times in
439 demosponges (Porifera): first insights from new mitogenomes and the inclusion of fossils in a birth-
440 death clock model. *BMC Evolutionary Biology*. 2018; 18: 114. [https://dx.doi.org/10.1186/s12862-](https://dx.doi.org/10.1186/s12862-018-1230-1)
441 [018-1230-1](#) PMID: [30021516](#)
- 442 8. Sibuet M, Olu K. Biogeography, biodiversity and fluid dependence of deep-sea cold-seep
443 communities at active and passive margins. *Deep-Sea Research II: Topical Studies in*
444 *Oceanography*. 1998; 45: 517–567.
- 445 9. Van Dover CL, German CR, Speer KG, Parson LM, Vrijenhoek RC. Evolution and Biogeography
446 of Deep-Sea Vent and Seep Invertebrates. *Science*. 2002; 295: 1253–1257. [https://doi.org/10.1126](https://doi.org/10.1126/science.1067361)
447 [/science.1067361](#) PMID: [11847331](#)
- 448 10. Martin W, Baross J, Kelley D, Russell MJ. Hydrothermal vents and the origin of life. *Nature*
449 *Review Microbiology*. 2008; 6: 805–814. <https://doi.org/10.1038/nrmicro1991> PMID:
450 [18820700](#)
- 451 11. Vrijenhoek RC. Genetic diversity and connectivity of deep-sea hydrothermal vent metapopulations.
452 *Molecular Ecology*. 2010; 19: 4391–4411. <https://doi.org/10.1111/j.1365-294X.2010.04789.x>
453 PMID: [20735735](#)
- 454 12. Sun J, Zhang Y, Xu T, Zhang Y, Mu H, Zhang Y, et al. Adaptation to deep-sea chemosynthetic env
455 ironments as revealed by mussel genomes. *Nature Ecology Evolution*. 2017; 1: 121. [https://doi.org](https://doi.org/10.1038/s41559-017-0121)
456 [/10.1038/s41559-017-0121](#) PMID: [28812709](#)
- 457 13. Zheng P, Wang MX, Li CL, Sun XQ, Wang XC, Sun Y, et al. Insights into deep-sea adaptations an
458 d host-symbiont interactions: A comparative transcriptome study on *Bathymodiolus* mussels and t

- 459 heir coastal relatives. *Molecular Ecology*. 2017; 26: 5133–5148. <https://doi.org/10.1111/mec.14160> PMID: [28437568](https://pubmed.ncbi.nlm.nih.gov/28437568/)
- 460
- 461 14. Hui M, Cheng J, Sha ZL. First comprehensive analysis of lysine acetylation in *Alvinocaris longiros*
- 462 *tris* from the deep-sea hydrothermal vents. *BMC Genomics*. 2018; 19: 352. <https://doi.org/10.1186/s12864-018-4745-3> PMID: [29747590](https://pubmed.ncbi.nlm.nih.gov/29747590/)
- 463
- 464 15. Lan Y, Sun J, Xu T, Chen C, Tian RM, Qiu JW, et al. *De novo* transcriptome assembly and positive
- 465 selection analysis of an individual deep-sea fish. *BMC Genomics*. 2018; 19: 394. <https://doi.org/10.1186/s12864-018-4720-z> PMID: [29793428](https://pubmed.ncbi.nlm.nih.gov/29793428/)
- 466
- 467 16. Gu ML, Dong XQ, Shi L, Shi L, Lin KQ, Huang XQ, et al. Differences in mtDNA whole sequence
- 468 between Tibetan and Han populations suggesting adaptive selection to high altitude. *Gene*. 2012;
- 469 496: 37–44. <https://doi.org/10.1016/j.gene.2011.12.016> PMID: [22233893](https://pubmed.ncbi.nlm.nih.gov/22233893/)
- 470
- 471 17. Yu L, Wang XP, Ting N, Zhang YP. Mitogenomic analysis of Chinese snub-nosed monkeys:
- 472 Evidence of positive selection in NADH dehydrogenase genes in high-altitude adaptation. *Mitochondrion*. 2011; 11: 497–503. <https://doi.org/10.1016/j.mito.2011.01.004> PMID: [21292038](https://pubmed.ncbi.nlm.nih.gov/21292038/)
- 473
- 474 18. Xu SQ, Yang YZ, Zhou J, Jin GE, Chen YT, Wang J, et al. A mitochondrial genome sequence of
- 475 the Tibetan antelope (*Pantholops hodgsonii*). *Genomics, proteomics & bioinformatics*. 2005; 3: 5–
- 476 17. PMID: [16144518](https://pubmed.ncbi.nlm.nih.gov/16144518/)
- 477
- 478 19. Ning T, Xiao H, Li J, Hua S, Zhang YP. Adaptive evolution of the mitochondrial ND6 gene in the
- 479 domestic horse. *Genetics and Molecular Research*. 2010; 9: 144–150. <https://doi.org/10.4238/vol9-1gmr705> PMID: [20198570](https://pubmed.ncbi.nlm.nih.gov/20198570/)
- 480
- 481 20. Wang ZF, Yonezawa T, Liu B, Ma T, Shen X, Su JP, et al. Domestication relaxed selective
- 482 constraints on the yak mitochondrial genome. *Molecular Biology and Evolution*. 2011; 28:
- 483 1553–1556. <https://doi.org/10.1093/molbev/msq336> PMID: [21156878](https://pubmed.ncbi.nlm.nih.gov/21156878/)
- 484
- 485 21. Zhou TC, Shen XJ, Irwin DM, Shen YY, Zhang YP. Mitogenomic analyses propose positive
- 486 selection in mitochondrial genes for high-altitude adaptation in galliform birds. *Mitochondrion*.
- 487 2014; 18: 70–75. <https://doi.org/10.1016/j.mito.2014.07.012> PMID: [25110061](https://pubmed.ncbi.nlm.nih.gov/25110061/)
- 488
- 489 22. Wang Y, Shen YJ, Feng CG, Zhao K, Song ZB, Zhang YP, et al. Mitogenomic perspectives on the
- 490 origin of Tibetan loaches and their adaptation to high altitude. *Scientific Reports*. 2016; 6: 29690. <https://doi.org/10.1038/srep29690> PMID: [27417983](https://pubmed.ncbi.nlm.nih.gov/27417983/)

- 488 23. Boss KJ, Turner RD. The giant white clam from the Galapagos Rift, *Calyptogena magnifica*
489 species novum. Malacologia. 1980; 20: 161–194.
- 490 24. Bennett BA, Smith CR, Glaser B, Maybaum HL. Faunal community structure of
491 achemoautotrophic assemblage on whale bones in the deep northeast Pacific Ocean. Marine
492 Ecology Progress. 1994; 108: 205–223.
- 493 25. Cosel RV, Salas C, Høisæter T. Vesicomidae (Mollusca: Bivalvia) of the genera *Vesicomya*,
494 *Wais-iuconcha*, *Isorropodon* and *Callogonia* in the eastern Atlantic and the Mediterranean. Sarsia,
495 86(4-5): 333-366. <https://doi.org/10.1080/00364827.2001.10425523>
- 496 26. Krylova EM, Sahling H. Vesicomidae (bivalvia): Current taxonomy and distribution. PLoS One.
497 2010; 5: e9957. <https://doi.org/10.1371/journal.pone.0009957> PMID: [20376362](https://pubmed.ncbi.nlm.nih.gov/20376362/)
- 498 27. Fisher CR. Chemoautotrophic and methanotrophic symbioses in marine invertebrates. Reviews in
499 Aquatic Sciences. 1990; 2: 399–436.
- 500 28. Krylova EM, Drozdov AL, Mironov AN. Presence of bacteria in gills of hadal bivalve “*Vesicomya*”
501 *sergeevi* Filatova, 1971. Ruthenica. 2000; 10: 76–79.
- 502 29. Chen C, Okutani T, Liang QY, Qiu JW. A Noteworthy New Species of the Family Vesicomidae
503 from the South China Sea (Bivalvia: Glossoidea). Venus. 2018; 76: 29–37.
- 504 30. Liu HL, Cai SY, Zhang HB, Vrijenhoek RC. Complete mitochondrial genome of hydrothermal vent
505 clam *Calyptogena magnifica*. Mitochondrial DNA Part A DNA Mapping, Sequencing, and
506 Analysis. 2015; 27: 4333–4335. <https://doi.org/10.3109/19401736.2015.1089488> PMID: [26462964](https://pubmed.ncbi.nlm.nih.gov/26462964/)
- 507 31. Liu HL, Cai SY, Liu J, Zhang HB. Comparative mitochondrial genomic analyses of three
508 chemosynthetic vesicomid clams from deep-sea habitats. Ecology and Evolution. 2018; 8: 7261–
509 7272. <https://doi.org/10.1002/ece3.4153> PMID: [30151147](https://pubmed.ncbi.nlm.nih.gov/30151147/)
- 510 32. Ozawa G, Shimamura S, Takaki Y, Takishita K, Ikuta T, Barry JP, et al. Ancient occasional
511 host switching of maternally transmitted bacterial symbionts of chemosynthetic vesicomid
512 clams. Genome Biology and Evolution. 2017; 9: 2226–2236. <https://doi.org/10.1093/gbe/evx166>
513 PMID: [28922872](https://pubmed.ncbi.nlm.nih.gov/28922872/)
- 514 33. Ozawa G, Shimamura S, Takaki Y, Yokobori SI, Ohara Y, Takishita K, et al. Updated
515 mitochondrial phylogeny of Pteriomorph and Heterodont Bivalvia, including deep-sea
516 chemosymbiotic *Bathymodiolus* mussels, vesicomid clams and the thyasirid clam *Conchocele cf.*

- 517 *bisecta*. Marine Genomics. 2017; 31: 43–52. <https://doi.org/10.1016/j.margen.2016.09.003> PMID:
518 [27720682](https://pubmed.ncbi.nlm.nih.gov/27720682/)
- 519 **34.** Luo RB, Liu BH, Xie YL, Li ZY, Huang WH, Yuan JY, et al. SOAPdenovo2: an empirically impro-
520 ved memory-efficient short-read *de novo* assembler. Giga Science. 2012; 1: 18. <https://doi.org/10.1186/2047-217X-1-18> PMID: [23587118](https://pubmed.ncbi.nlm.nih.gov/23587118/)
- 522 **35.** Haas BJ, Salzberg SL, Zhu W, Pertea M, Allen JE, Orvis J et al. Automated eukaryotic gene
523 structure annotation using EVIDENCEModeler and the Program to Assemble Spliced Alignments.
524 Genome Biology. 2008; 9: R7. <https://doi.org/10.1186/gb-2008-9-1-r7> PMID: [18190707](https://pubmed.ncbi.nlm.nih.gov/18190707/)
- 525 **36.** Lagesen K, Hallin P, Rødland EA, Stærfeldt HH, Rognes T, Ussery DW. RNAmmer: consistent
526 and rapid annotation of ribosomal RNA genes. Nucleic Acids Research. 2007; 35: 3100–3108.
527 <https://doi.org/10.1093/nar/gkm160> PMID: [17452365](https://pubmed.ncbi.nlm.nih.gov/17452365/)
- 528 **37.** Lowe TM, Eddy SR. tRNAscan-SE: a program for improved detection of transfer RNA genes in
529 genomic sequence. Nucleic Acids Research. 1997; 25: 955–964. <https://doi.org/10.1093/nar/25.5.955> PMID: [9023104](https://pubmed.ncbi.nlm.nih.gov/9023104/)
- 531 **38.** Lohse M, Drechsel O, Bock R. OrganellarGenomeDRAW (OGDRAW): a tool for the easy
532 generation of high-quality custom graphical maps of plastid and mitochondrial genomes. Current
533 Genetics. 2007; 52: 267–274. <https://doi.org/10.1007/s00294-007-0161-y> PMID: [17957369](https://pubmed.ncbi.nlm.nih.gov/17957369/)
- 534 **39.** Librado P, Rozas J. DnaSP v5: A software for comprehensive analysis of DNA polymorphism data.
535 Bioinformatics. 2009; 25: 1451–1452. <https://doi.org/10.1093/bioinformatics/btp187> PMID:
536 [19346325](https://pubmed.ncbi.nlm.nih.gov/19346325/)
- 537 **40.** Perna NT, Kocher TD. Patterns of nucleotide composition at fourfold degenerate sites of animal
538 mitochondrial genomes. Journal of Molecular Evolution. 1995; 41: 353–358. PMID: [7563121](https://pubmed.ncbi.nlm.nih.gov/7563121/)
- 539 **41.** Benson G. Tandem repeats finder: a program to analyze DNA sequences. Nucleic Acids Research.
540 1999; 27: 573–580. <https://doi.org/10.1093/nar/27.2.573> PMID: [9862982](https://pubmed.ncbi.nlm.nih.gov/9862982/)
- 541 **42.** Zuker M. Mfold web server for nucleic acid folding and hybridization prediction. Nucleic Acids
542 Research. 2003; 31: 3406–3415. <https://doi.org/10.1093/nar/gkg595> PMID: [12824337](https://pubmed.ncbi.nlm.nih.gov/12824337/)
- 543 **43.** Talavera G, Castresana J. Improvement of phylogenies after removing divergent and ambiguously
544 aligned blocks from protein sequence alignments. Systematic Biology. 2007; 56: 564–577.
545 <https://doi.org/10.1080/10635150701472164> PMID: [17654362](https://pubmed.ncbi.nlm.nih.gov/17654362/)

- 546 **44.** Darriba D, Taboada GL, Doallo R, Posada D. jModelTest 2: more models, new heuristics and
547 parallel computing. *Nature Methods*. 2012; 9: 772. <https://doi.org/10.1038/nmeth.2109> PMID:
548 [22847109](https://pubmed.ncbi.nlm.nih.gov/22847109/)
- 549 **45.** Darriba D, Taboada GL, Doallo R, Posada D. ProfTest 3: fast selection of best-fit models of protein
550 evolution. *Bioinformatics*. 2011; 27: 1164–1165. <https://doi.org/10.1093/bioinformatics/btr088>
551 PMID: [21335321](https://pubmed.ncbi.nlm.nih.gov/21335321/)
- 552 **46.** Stamatakis A. RAxML version 8: a tool for phylogenetic analysis and post-analysis of large
553 phylogenies. *Bioinformatics*. 2014; 30: 1312–1313. <https://doi.org/10.1093/bioinformatics/btu033>
554 PMID: [24451623](https://pubmed.ncbi.nlm.nih.gov/24451623/)
- 555 **47.** Ronquist F, Teslenko M, van der Mark P, Ayres DL, Darling A, Höhna S. MrBayes 3.2: efficient
556 bayesian phylogenetic inference and model choice across a large model space. *Systematic Biology*.
557 2012; 61: 539–542. <https://doi.org/10.1093/sysbio/sys029> PMID: [22357727](https://pubmed.ncbi.nlm.nih.gov/22357727/)
- 558 **48.** Ohta T. The nearly neutral theory of molecular evolution. *Annual Review of Ecology and*
559 *Systematics*. 1992; 23: 263–286. <https://www.jstor.org/stable/2097289>
- 560 **49.** Yang Z. PAML 4: a program package for phylogenetic analysis by maximum likelihood. *Molecular*
561 *Biology and Evolution*. 2007; 24: 1586–1591. <https://doi.org/10.1093/molbev/msm088> PMID:
562 [17483113](https://pubmed.ncbi.nlm.nih.gov/17483113/)
- 563 **50.** Yang Z, Nielsen R, Goldman N, Pedersen AM. Codon-substitution models for heterogeneous
564 selection pressure at amino acid sites. *Genetics*. 2000; 155: 431–449. PMID: [10790415](https://pubmed.ncbi.nlm.nih.gov/10790415/)
- 565 **51.** Nielsen R, Yang Z. Likelihood models for detecting positively selected amino acid sites and
566 applications to the HIV-1 envelope gene. *Genetics*. 1998; 148: 929–936. PMID: [9539414](https://pubmed.ncbi.nlm.nih.gov/9539414/)
- 567 **52.** Yang Z. Likelihood ratio tests for detecting positive selection and application to primate lysozyme
568 evolution. *Molecular Biology and Evolution*. 1998; 15: 568–573. <https://doi.org/10.1093/oxfordjournals.molbev.a025957> PMID: [9580986](https://pubmed.ncbi.nlm.nih.gov/9580986/)
- 569 [nals.molbev.a025957](https://pubmed.ncbi.nlm.nih.gov/9580986/) PMID: [9580986](https://pubmed.ncbi.nlm.nih.gov/9580986/)
- 570 **53.** Yang Z, Wong WS, Nielsen, R. Bayes empirical bayes inference of amino acid sites under positive
571 selection. *Molecular Biology and Evolution*. 2005; 22: 1107–1118. [https://doi.org/10.1093/molbev/](https://doi.org/10.1093/molbev/msi097)
572 [msi097](https://pubmed.ncbi.nlm.nih.gov/15689528/) PMID: [15689528](https://pubmed.ncbi.nlm.nih.gov/15689528/)
- 573 **54.** Xu X, Wu X, Yu Z. The mitogenome of *Paphia euglypta* (Bivalvia: Veneridae) and comparative mi
574 togenomic analyses of three venerids. *Genome*. 2010; 53: 1041–1052. [https://doi.org/10.1139/G10-](https://doi.org/10.1139/G10-096)
575 [096](https://pubmed.ncbi.nlm.nih.gov/21164537/) PMID: [21164537](https://pubmed.ncbi.nlm.nih.gov/21164537/)

- 576 **55.** Liao F, Wang L, Wu S, Li YP, Zhao L, Huang GM, et al. The complete mitochondrial genome of
577 the fall webworm, *Hyphantria cunea* (Lepidoptera: Arctiidae). International Journal of Biological
578 Sciences. 2010; 6: 172–186. PMID: [20376208](#)
- 579 **56.** Wang ZL, Chao L, Fang WY, Yu XP. The Complete Mitochondrial Genome of two *Tetragnatha*
580 Spiders (Araneae: Tetragnathidae): Severe Truncation of tRNAs and Novel Gene Rearrangements
581 in Araneae. International Journal of Biological Sciences. 2016; 12: 109–119. <https://doi.org/10.7150/ijbs.12358> 12358 PMID: [26722222](#)
- 582
- 583 **57.** Ojala D, Montoya J, Attardi G. tRNA punctuation model of RNA processing in human
584 mitochondria. Nature. 1981; 290: 470–474. PMID: [7219536](#)
- 585 **58.** Dreyer H, Steiner G. The complete sequences and gene organisation of the mitochondrial genome
586 of the heterodont bivalves *Acanthocardia tuberculata* and *Hiatella arctica* – and the first record for
587 a putative *Atpase subunit 8* gene in marine bivalves. Frontiers in Zoology. 2006; 3: 13. [https://dx.d](https://dx.doi.org/10.1186/1742-9994-3-13)
588 [oi.org/10.1186/1742-9994-3-13](https://dx.doi.org/10.1186/1742-9994-3-13) PMID: [16948842](#)
- 589 **59.** Salvato P, Simonato M, Battisti A, Negrisolto E. The complete mitochondrial genome of the
590 bag-shelter moth *Ochrogaster lunifer* (Lepidoptera, Notodontidae). BMC Genomics. 2008; 9: 331.
591 <https://dx.doi.org/10.1186/1471-2164-9-331> PMID: [18627592](#)
- 592 **60.** Yu H, Li Q. Complete mitochondrial DNA sequence of *Crassostrea nippona*: comparative and
593 phylogenomic studies on seven commercial *Crassostrea* species. Molecular Biology Reports. 2012;
594 39: 999–1009. <https://doi.org/10.1007/s11033-011-0825-z> PMID: [21562763](#).
- 595 **61.** Sun SE, Sha ZL, Wang YR. Complete mitochondrial genome of the first deep-sea spongiolid
596 shrimp *Spongiocaris panglao* (Decapoda: Stenopodidea): Novel gene arrangement and the
597 phylogenetic position and origin of Stenopodidea. Gene. 2018; 676: 123–138. [https://doi.org/10.10](https://doi.org/10.1016/j.gene.2018.07.026)
598 [16/j.gene.2018.07.026](https://doi.org/10.1016/j.gene.2018.07.026) PMID: [30021129](#)
- 599 **62.** Brown WM. The mitochondrial genome of animals. In: Molecular Evolutionary Genetics. New
600 York: Plenum Press; 1985.
- 601 **63.** Chai HN, Du YZ, Zhai BP. Characterization of the complete mitochondrial genome of
602 *Cnaphalocrocis medinalis* and *Chilo suppressalis* (Lepidoptera: Pyralidae). International Journal of
603 Biological Sciences. 2012; 8: 561–579. <https://doi.org/10.1007/s10126-005-0004-0> PMID:
604 [16132463](#)
- 605 **64.** Zhang B, Zhang YH, Wang X, Zhang HX, Lin Q. The mitochondrial genome of a sea anemone

- 606 *Bolocera sp.* exhibits novel genetic structures potentially involved in adaptation to the seep-sea
607 environment. *Ecology and Evolution*. 2017; 7: 4951–4962. <https://doi.org/10.1002/ece3.3067>
608 PMID: [28690821](https://pubmed.ncbi.nlm.nih.gov/28690821/)
- 609 65. Sun SE, Hui M, Wang MX, Sha ZL. The complete mitochondrial genome of the alvinocaridid
610 shrimp *Shinkaicaris leurokolos* (Decapoda, Caridea): Insight into the mitochondrial genetic basis of
611 deep-sea hydrothermal vent adaptation in the shrimp. *Comparative Biochemistry and Physiology-*
612 *Part D*. 2018; 25: 42–52. <https://doi.org/10.1016/j.cbd.2017.11.002> PMID: [29145028](https://pubmed.ncbi.nlm.nih.gov/29145028/)
- 613 66. Plazzi F, Ribani A, Passamonti M. The complete mitochondrial genome of *Solemya velum* (Mollusc
614 a: Bivalvia) and its relationships with conchifera. *BMC Genomics*. 2013; 14: 409. <https://doi.org/10.1186/1471-2164-14-409> PMID: [23777315](https://pubmed.ncbi.nlm.nih.gov/23777315/)
- 616 67. Okimoto R, Macfarlane JL, Clary DO, Wolstenholme DR. The mitochondrial genomes of
617 two nematodes, *Caenorhabditis elegans* and *Ascaris suum*. *Genetics*. 1992; 130: 471–498. PMID:
618 [1551572](https://pubmed.ncbi.nlm.nih.gov/1551572/)
- 619 68. Ohtsuki T, Kawai G, Watanabe K. The minimal tRNA: unique structure of *Ascaris suum*
620 mitochondrial tRNA(Ser)(UCU) having a short T arm and lacking the entire D arm. *FEBS Letter*.
621 2002; 514: 37–43. PMID: [11904178](https://pubmed.ncbi.nlm.nih.gov/11904178/)
- 622 69. Chinnaronk S, Gravers Jeppesen M, Suzuki T, Nyborg J, Watanabe K. Dualmode recognition of
623 noncanonical tRNAs(Ser) by seryl-tRNA synthetase in mammalian mitochondria. *Embo Journal*.
624 2005; 24: 3369–3379. <https://doi.org/10.1038/sj.emboj.7600811> PMID: [16163389](https://pubmed.ncbi.nlm.nih.gov/16163389/)
- 625 70. Lavrov DV, Brown WM, Boore JL. A novel type of RNA editing occurs in the mitochondrial
626 tRNAs of the centipede *Lithobius forficatus*. *Proceedings of the National Academy of Sciences of*
627 *the United States of America*. 2000; 97: 13738–13742. <https://doi.org/10.1073/pnas.250402997>
628 PMID: [11095730](https://pubmed.ncbi.nlm.nih.gov/11095730/)
- 629 71. Miller AD, Murphy NP, Burrige CP, Austin CM. Complete mitochondrial DNA sequences of
630 the decapod crustaceans *Pseudocarcinus gigas* (Menippidae) and *Macrobrachium rosenbergii*
631 (Palaemonidae). *Marine Biotechnology*. 2005; 7: 339–349. [https://doi.org/10.1007/s10126-004-](https://doi.org/10.1007/s10126-004-4077-y)
632 [4077-y](https://doi.org/10.1007/s10126-004-4077-y) PMID: [15902543](https://pubmed.ncbi.nlm.nih.gov/15902543/)
- 633 72. Aquadro CF, Greenberg BD. Human mitochondrial DNA variation and evolution: Analysis of
634 nucleotide sequences from seven individuals. *Genetics*. 1983; 103: 287–312.

- 635 73. Marshall HD, Baker AJ. Structural conservation and variation in the mitochondrial control region
636 of fringilline finches (*Fringilla* spp.) and the greenfinch (*Carduelis chloris*). *Molecular Biology and*
637 *Evolution*. 1997; 14: 173–184. <https://doi.org/10.1093/oxfordjournals.molbev.a025750> PMID:
638 [9029795](https://pubmed.ncbi.nlm.nih.gov/9029795/)
- 639 74. Flot JF, Tillier S. The mitogenome of *Pocillopora* (Cnidaria: Scleractinia) contains two variable
640 regions: The putative D-loop and a novel ORF of unknown function. *Gene*. 2007; 401: 80–87. [https://](https://doi.org/10.1016/j.gene.2007.07.006)
641 doi.org/10.1016/j.gene.2007.07.006 PMID: [17716831](https://pubmed.ncbi.nlm.nih.gov/17716831/)
- 642 75. Stanton DJ, Daehler LL, Moritz CC, Brown WM. Sequences with the potential to form stem-and-
643 loop structures are associated with coding-region duplications in animal mitochondrial DNA.
644 *Genetics*. 1994; 137: 233–241. PMID: [8056313](https://pubmed.ncbi.nlm.nih.gov/8056313/)
- 645 76. Fernández-Silva P, Enriquez JA, Montoya J. Replication and transcription of mammalian
646 mitochondrial DNA. *Experimental Physiology*. 2003; 88: 41–56. PMID: [12525854](https://pubmed.ncbi.nlm.nih.gov/12525854/)
- 647 77. Serb JM, Lydeard C. Complete mtDNA sequence of the north American freshwater mussel,
648 *Lampsilis ornata* (Unionidae): an examination of the evolution and phylogenetic utility of
649 mitochondrial genome organization in Bivalvia (Mollusca). *Molecular Biology and Evolution*. 2003;
650 20: 1854–1866. <https://doi.org/10.1093/molbev/msg218> PMID: [12949150](https://pubmed.ncbi.nlm.nih.gov/12949150/)
- 651 78. Ren J, Shen X, Jiang F, Liu B. The mitochondrial genomes of two scallops, *Argopecten irradians*
652 and *Chlamys farreri* (Mollusca: Bivalvia): the most highly rearranged gene order in the family
653 Pectinidae. *Journal of Molecular Evolution*. 2009; 70: 57–68. [https://doi.org/10.1007/s00239-009-](https://doi.org/10.1007/s00239-009-9308-4)
654 [9308-4](https://doi.org/10.1007/s00239-009-9308-4) PMID: [20013337](https://pubmed.ncbi.nlm.nih.gov/20013337/)
- 655 79. Milbury CA, Gaffney PM. Complete mitochondrial DNA sequence of the eastern oyster
656 *Crassostrea virginica*. *Marine Biotechnology*. 2005; 7: 697–712. [https://doi.org/10.1007/s10126-](https://doi.org/10.1007/s10126-005-0004-0)
657 [005-0004-0](https://doi.org/10.1007/s10126-005-0004-0) PMID: [16132463](https://pubmed.ncbi.nlm.nih.gov/16132463/)
- 658 80. Kumazawa Y, Miura S, Yamada C, Hashiguchi Y. Gene rearrangements in gekkonid mitochondrial
659 genomes with shuffling, loss, and reassignment of tRNA genes. *BMC Genomics*. 2014; 15: 930.
660 <https://doi.org/10.1186/1471-2164-15-930> PMID: [25344428](https://pubmed.ncbi.nlm.nih.gov/25344428/)
- 661 81. Sahyoun AH, Hölzer M, Jühling F, Hölzer zu Siederdisen C, Al-Arab M, Tout K, et al. Towards a
662 comprehensive picture of alloacceptor tRNA remodeling in metazoan mitochondrial genomes.
663 *Nucleic Acids Research*. 2015; 43: 8044–8056. <https://doi.org/10.1093/nar/gkv746> PMID:
664 [26227972](https://pubmed.ncbi.nlm.nih.gov/26227972/)

- 665 **82.** Boore JL, Brown WM. Big trees from little genomes: mitochondrial gene order as a phylogenetic
666 tool. *Current Opinion in Genetics and Development*. 1998; 8: 668–674. PMID: [9914213](#)
- 667 **83.** Perseke M, Bernhard D, Fritsch G, Brümmer F, Stadler PF, Schlegel M. Mitochondrial genome ev
668 olution in Ophiuroidea, Echinoidea, and Holothuroidea: insights in phylogenetic relationships of Ec
669 hinodermata. *Molecular Phylogenetic Evolution*. 2010; 56:201–211. [https://doi.org/10.1016/j.ympev.](https://doi.org/10.1016/j.ympev.2010.01.035)
670 [2010.01.035](https://doi.org/10.1016/j.ympev.2010.01.035) PMID: [20152912](#)
- 671 **84.** Krylova EM, Sahling H. Recent bivalve molluscs of the genus *Calypptogena* (Vesicomidae).
672 *Journal of Molluscan Studies*. 2006; 72: 359–395. <https://doi.org/10.1093/mollus/eyl022>
- 673 **85.** Decker C, Olu K, Cunha RL, Arnaud-Haond S. Phylogeny and diversification patterns among vesico
674 myid bivalves. *PLoS ONE*. 2012; 7: e33359. <https://doi.org/10.1371/journal.pone.0033359> PMID:
675 22511920
- 676 **86.** Johnson SB, Krylova EM, Audzijonyte A, Sahling H, Vrijenhoek RC. Phylogeny and origins of che
677 mosynthetic vesicomid clams. *Systematics and Biodiversity*. 2017; 15: 346–360. [https://doi.org/10.1](https://doi.org/10.1080/14772000.2016.1252438)
678 [080/14772000.2016.1252438](https://doi.org/10.1080/14772000.2016.1252438)
- 679 **87.** Shen YY, Liang L, Zhu ZH, Zhou WP, Irwin DM, Zhang YP. Adaptive evolution of energy
680 metabolism genes and the origin of flight in bats. *Proceedings of the National Academy of Sciences*
681 *of the United States of America*. 2010; 107: 8666–8671. <https://doi.org/10.1073/pnas.0912613107>
682 PMID: [20421465](#)
- 683 **88.** Tomasco IH, Lessa EP. The evolution of mitochondrial genomes in subterranean caviomorph
684 rodents: adaptation against a background of purifying selection. *Molecular Phylogenetics and*
685 *Evolution*. 2011; 61: 64–70. <https://doi.org/10.1016/j.ympev.2011.06.014> PMID: [21723951](#)
- 686 **89.** Plazzi F, Puccio G, Passamonti M. Burrowers from the past: mitochondrial signatures of Ordovician
687 bivalve infaunalization. *Genome Biology and Evolution*. 2017; 9: 956–967. [https://doi.org/10.109](https://doi.org/10.1093/gbe/evx051)
688 [3/gbe/evx051](https://doi.org/10.1093/gbe/evx051) PMID: [28338965](#)
- 689 **90.** da Fonseca RR, Johnson WE, O'Brien SJ, Ramos MJ, Antunes A. The adaptive evolution of the
690 mammalian mitochondrial genome. *BMC Genomics*. 2008; 9: 119. [https://doi.org/10.1186/1471-](https://doi.org/10.1186/1471-2164-9-119)
691 [2164-9-119](https://doi.org/10.1186/1471-2164-9-119) PMID: [18318906](#)
- 692 **91.** Yang YX, Xu SX, Xu JX, Guo Y, Yang G. Adaptive evolution of mitochondrial energy metabolism
693 genes associated with increased energy demand in flying insects. *Plos ONE*. 2014; 9: e99120. <https://doi.org/10.1371/journal.pone.0099120> PMID: [24918926](#)
694 [/doi.org/10.1371/journal.pone.0099120](https://doi.org/10.1371/journal.pone.0099120)

- 695 **92.** Das J. The role of mitochondrial respiration in physiological and evolutionary adaptation.
696 BioEssays. 2006; 28: 890–901. <https://doi.org/10.1002/bies.20463> PMID: [16937356](https://pubmed.ncbi.nlm.nih.gov/16937356/)
- 697 **93.** Zhang J, Nielsen R, Yang Z. Evaluation of an improved branch-site likelihood method for detecting
698 positive selection at the molecular level. Molecular Biology and Evolution. 2005; 22: 2472–2479. <https://doi.org/10.1093/molbev/msi237> PMID: [16107592](https://pubmed.ncbi.nlm.nih.gov/16107592/)
- 700 **94.** Trumpower BL. The protonmotive Q cycle. Energy transduction by coupling of proton
701 translocation to electron transfer by the cytochrome bc1 complex. Journal of Biological Chemistry.
702 1990; 265:11409–11412. PMID: [2164001](https://pubmed.ncbi.nlm.nih.gov/2164001/)
- 703 **95.** Silva G, Lima FP, Martel P, Caastilho R. Thermal adaptation and clinal mitochondrial DNA variati
704 on of European anchovy. Proceedings Biological Sciences. 2014; 281: 1792. <https://doi.org/10.1098/rspb.2014.1093> PMID: [25143035](https://pubmed.ncbi.nlm.nih.gov/25143035/)
- 706 **96.** Luo YJ, Gao WX, Gao YQ, Tang S, Huang QY, Tan XL, et al. Mitochondrial genome analysis of
707 *Ochotona curzoniae* and implication of cytochrome c oxidase in hypoxic adaptation.
708 Mitochondrion. 2008; 8: 352–357. <https://doi.org/10.1016/j.mito.2008.07.005> PMID: [18722554](https://pubmed.ncbi.nlm.nih.gov/18722554/)
- 709 **97.** Mahalingam S, McClelland GB, Scott GR. Evolved changes in the intracellular distribution and
710 physiology of muscle mitochondria in high-altitude native deer mice. The Journal of Physiology.
711 2017; 595: 4785–4801. <https://doi.org/10.1113/JP274130> PMID: [28418073](https://pubmed.ncbi.nlm.nih.gov/28418073/)
- 712 **98.** Mu WD, Liu J, Zhang HB. Complete mitochondrial genome of *Benthodytes marianensis*
713 (Holothuroidea: Elapsozoa: Psychropotidae): Insight into deep sea adaptation in the sea cucumber.
714 PLoS ONE. 2018; 13: e0208051. <https://doi.org/10.1371/journal.pone.0208051> PMID: [30500836](https://pubmed.ncbi.nlm.nih.gov/30500836/)
- 715 **99.** Mu WD, Liu J, Zhang HB. The first complete mitochondrial genome of the Mariana Trench
716 *Freyastera benthophila* (Asterozoa: Brisingida: Brisingidae) allows insights into the deep-sea
717 adaptive evolution of Brisingida. Ecology and Evolution. 2018; 8: 10673-10686.
718 <https://doi.org/10.1002/ece3.4427> PMID: [30519397](https://pubmed.ncbi.nlm.nih.gov/30519397/)

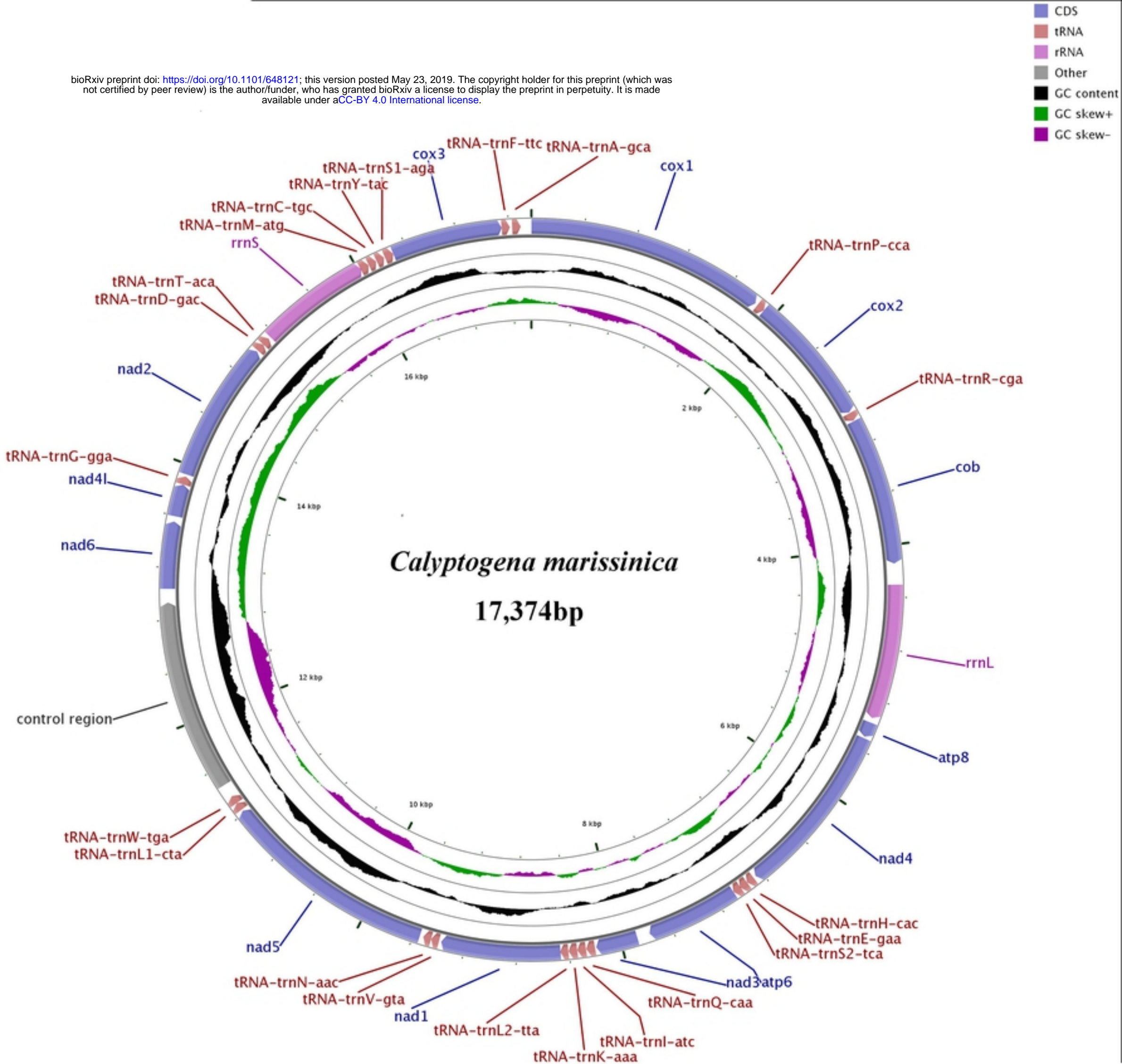


Figure 1

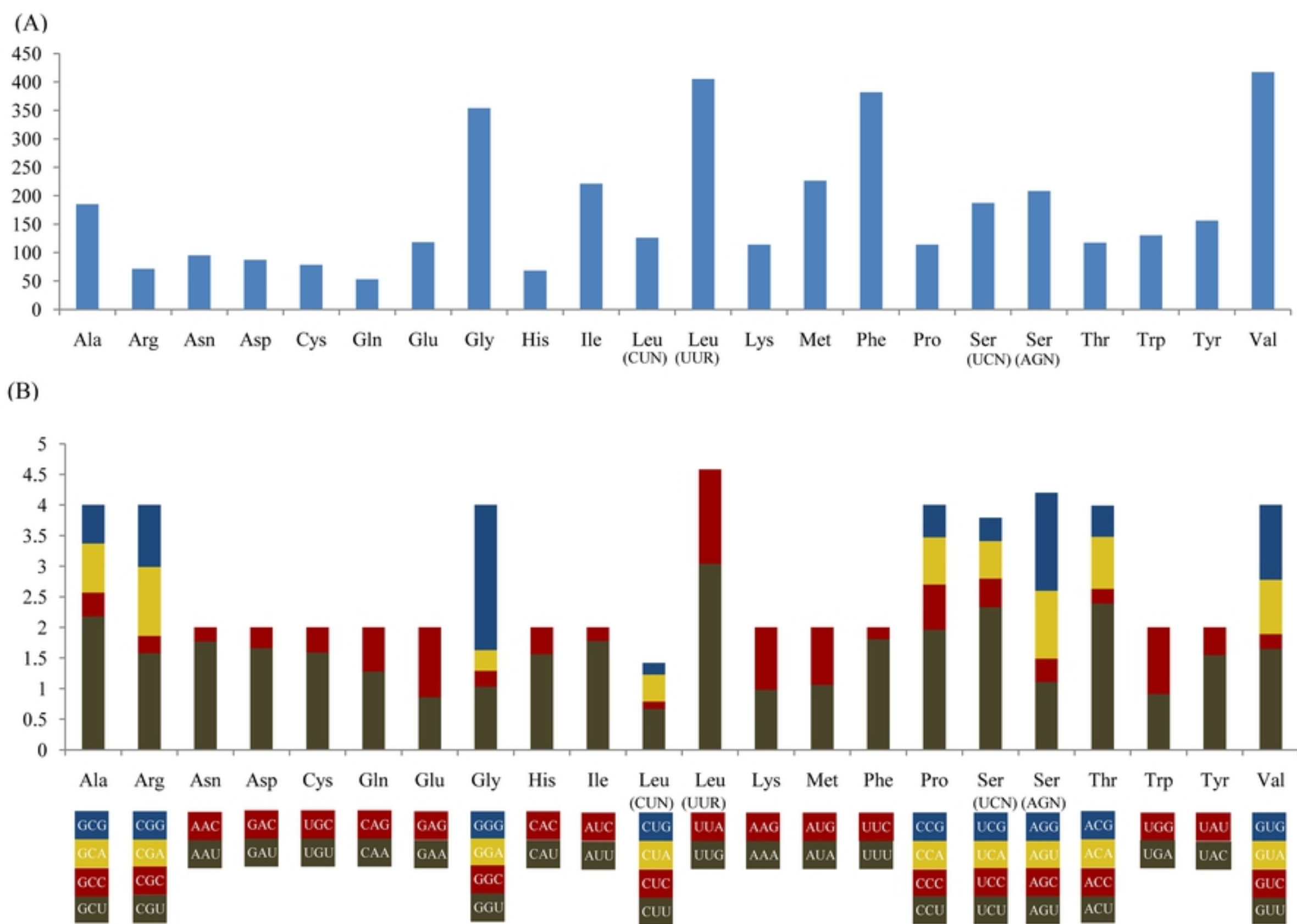


Figure 2

1 AGGTTTTTTTTTTTTTTCGTTGAAACTTAGCTGAGTAACAGGAGATTTTGTGGAATTGAA
61 AGAGGTTTACCCCCCTCTCTAAGTTAGTTAGAATTTTGTTTAAATTTTATATGGCCGACAA
121 ATGTAGCAATACAGCATATATGGTTATTTGGTTGGGGTACTTTATAGGAGTATGCCCA
181 TTGTAA[EAA]CTT[EAT]TACTTTGTTAAAAATGTCCTTAAATG[EAT]TATTGGT[EAT]GG
241 AAGGT[EAT]ATCACCTAGTCTCAAATTTCTCTTTAAGGAAGGGTGGTGTAAAAACATTTT
301 AAATGAGTTGGAGAAGGCCAA[EAT]FAGTATTAAGGAAGGAGAACTTTTCTTTTAACTTG
361 AATAGGTTAAACT[EAA]CAATTTGT[EAT]ACAGGTGGTTTGAGGGAGCAAGCTAGTGCTA
421 TTTGAAGAGTACTTTTGCCTTTAAAA[EAAA]ATTACCGGTATGTTTTCTTTTTCTTCA
481 TTTACTTAACAAG[EAT]CCCTGTAGAACTTACCAAGTGTGTGTGTGCAIGTGTTATATAT
541 **AT rich region**
ATATATATATAAAGTAAGG[EAT]CTAGTATAATTTATATATATATATATTTTACTCTTTAG
601 AGTAAAAATATATAATATAAATTAATACTA[EAA]CCCATACTTTATATATATATATATAT
661 ATATATATGIGTATTTCCCCACACCCACCCCTGG[EAAAA]ATAATTATAATTTT[EAT]TTTT
721 ACCAGGAGTGGGTGTGGG[EAA]ACACATATATATATATATAAATCAGCTTTTAGCT[EAT]T
781 TATATAATTTACTAAACTTTTTAAAAATTTTCA[EAAAAA]TAAAAATAATTAACTTAAATTT
841 T[EAAA]TAAATTTTTTTT[EAT]AAAAGTGTGTTTAAATATATTTATCTATCAAAA[EAAAAA]
901 AAAAT[EAT]CAGGCAGGCCTTGTATTCCCTTCCCAGCGTGGCTCCGTGAGGTCTGCCTTAC
961 GCCCAGTAAAGCCTGGGCCCTGTTTCCC[EAT]CATTTTTATTTTTTTTTTCTTTTAAATCGT
1021 AAATAAAACACCAGTAAACATTTTAAACATAAAGTTAGTGCCAACCTAAGTTTGGCACTAAT
1081 ATATATATGCATATTTACAAAATTTTCATTATTTTGTAAACAAAATAA[EAAAA]TGCTAA
1141 ATATTCCCCATGCTCCTATTTAATTAATTTTATAAATTAAGGAGTATGAAGAATATTTA
1201 GGTATTTTTTTTACTTCGTAAAAAATACATAAATAATATATATACAATACCTAAAATTTGTTA
1261 AACAAATTTAGGTATTGTATATATATTTAATAAAAAAAAAAAAAAAAAAATAGGTTTT[EAT]TTC
1321 [EAA]TGTAAACAAGGTAGACTTTAAAAATTTATACTAAAATGGAGGATATTTTAGGTTGG
1381 [EAAA]TAAATTCCAAGAGTTTTAGCATTTGTTTAAAAA[EAT]TTTTTATGTT[EAT]TTTC[EAT]
1441 [AT]TGTAAACAAGGTAGACTTTAAAAATTTATACTAAAATGGAG[EAT]TTTTTATGTT[EAT]
1501 [AA]TAAATTTCAAGAGTTTTAGCATTTGTTTAAAAA[EAT]TTTTTATGTT[EAT]TTTC[EAA]
1561 TGTAAACAAGGTAGACTTTAAAAATTTATACTAAAATGGAG[EAT]TTTTTATGTT[EAT]TTTC[EAA]
1621 TAAATTTCAAGAGTTTTAGCATTTGTTTAAAAA[EAT]TTTTTATGTT[EAT]TTTCGA—NAD6

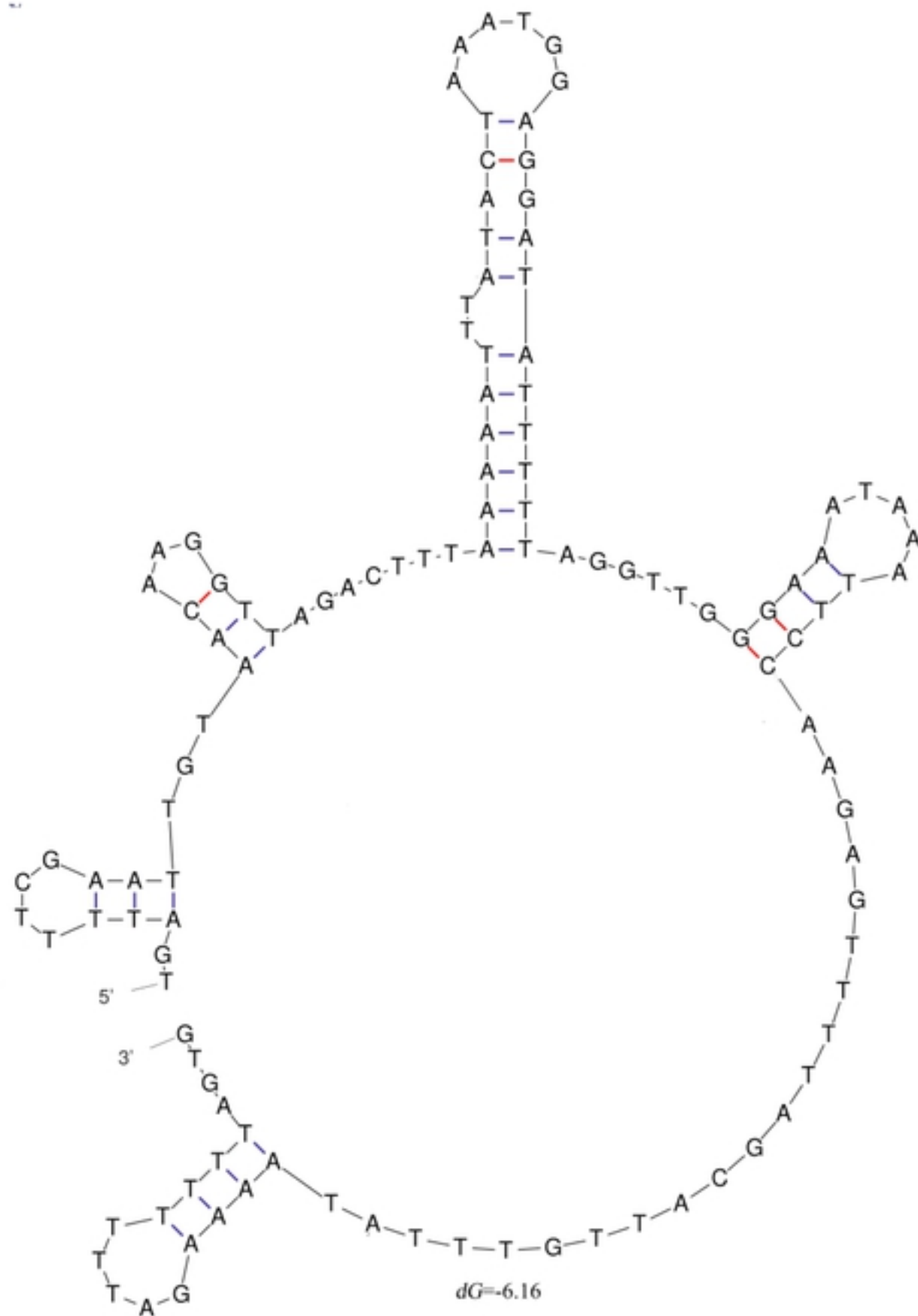


Figure 3

Panopea generosa
(Myoida: Hiatellidae)

cox1 CR cox2 V T nad4l atp8 nad4 H E S2 nad3 I D K L2 nad1 L1 N nad5 nad6 R cob W rml atp6 M rms cox3 S1 nad2 Q F C P G A

Moerella iridescens
(Veneroida: Tellinidae)

cox1 nad4 H S2 E nad3 I K nad4l Y T L2 D L1 nad1 N nad5 R cob cox2 V W G rms CR M S1 nad6 rml atp6 cox3 nad2 P Q C A F

Coelomactra antiquata
(Veneroida: Mactridae)

cox1 V W nad6 Q T nad1 G nad2 D P rms Y S cox3 cob rml nad4 H CR R L2 E atp6 nad3 K I nad5 cox2 nad4l N L1 C M F A

Meretrix meretrix
(Veneroida: Veneridae)

cox1 L2 nad1 nad2 nad4l I D cox2 P cob rml nad4 H E S2 atp6 nad3 nad5 nad6 W M V K F L1 G CR Q1 Q2 Q3 R N T rms C Y cox3 A

Abyssogena mariana
(Veneroida: Vesicomysidae)

cox1 P cox2 R cob rml atp8 nad4 H E S2 atp6 nad3 Q I K L2 nad1 V N nad5 L1 W CR nad6 nad4l G L3 nad2 D T rms M C Y S1 cox3 F A

Abyssogena phaseoliformis
(Veneroida: Vesicomysidae)

cox1 P cox2 R cob rml atp8 nad4 H E S2 atp6 nad3 Q I K L2 nad1 V N nad5 L1 W H2 CR nad6 nad4l G S3 nad2 D T rms M C Y S1 cox3 F A

Archivesica gigas
(Veneroida: Vesicomysidae)

cox1 P cox2 R cob rml atp8 nad4 H E S2 atp6 nad3 Q I K L2 nad1 V N nad5 L1 CR nad6 nad4l G nad2 D T rms M C Y S1 cox3 F A

Archivesica Sp.
(Veneroida: Vesicomysidae)

cox1 P cox2 R cob rml atp8 nad4 H E S2 atp6 nad3 Q I K L2 nad1 V N nad5 CR nad6 nad4l G nad2 D T rms M C Y S1 cox3 F A

Archivesica Pacific
Calyptogena magnifica
Calyptogena marissinica
(Veneroida: Vesicomysidae)

cox1 P cox2 R cob rml atp8 nad4 H E S2 atp6 nad3 Q I K L2 nad1 V N nad5 L1 W CR nad6 nad4l G nad2 D T rms M C Y S1 cox3 F A

Isorropodon fossajaponicum
(Veneroida: Vesicomysidae)

cox1 N2 P cox2 R cob rml atp8 nad4 H E S2 atp6 nad3 Q I K L2 nad1 V N nad5 L1 W K2 CR nad6 nad4l G nad2 D T rms M C Y S1 cox3 F A

Phreagena okutanii
(Veneroida: Vesicomysidae)

cox1 P cox2 R cob rml atp8 nad4 H E S2 atp6 nad3 Q I K L2 nad1 V N nad5 L1 W CR nad6 nad4l G M2 nad2 D T rms M C Y S1 cox3 F A

Figure 4

Colored ranges

- Pectinidae
- Lucinidae
- Cardiidae
- Hiatellidae
- Solenidae
- Donacidae
- Semelidae
- Tellinidae
- Psammobiidae
- Solecurtidae
- Mactridae
- Veneridae
- Vesicomysidae

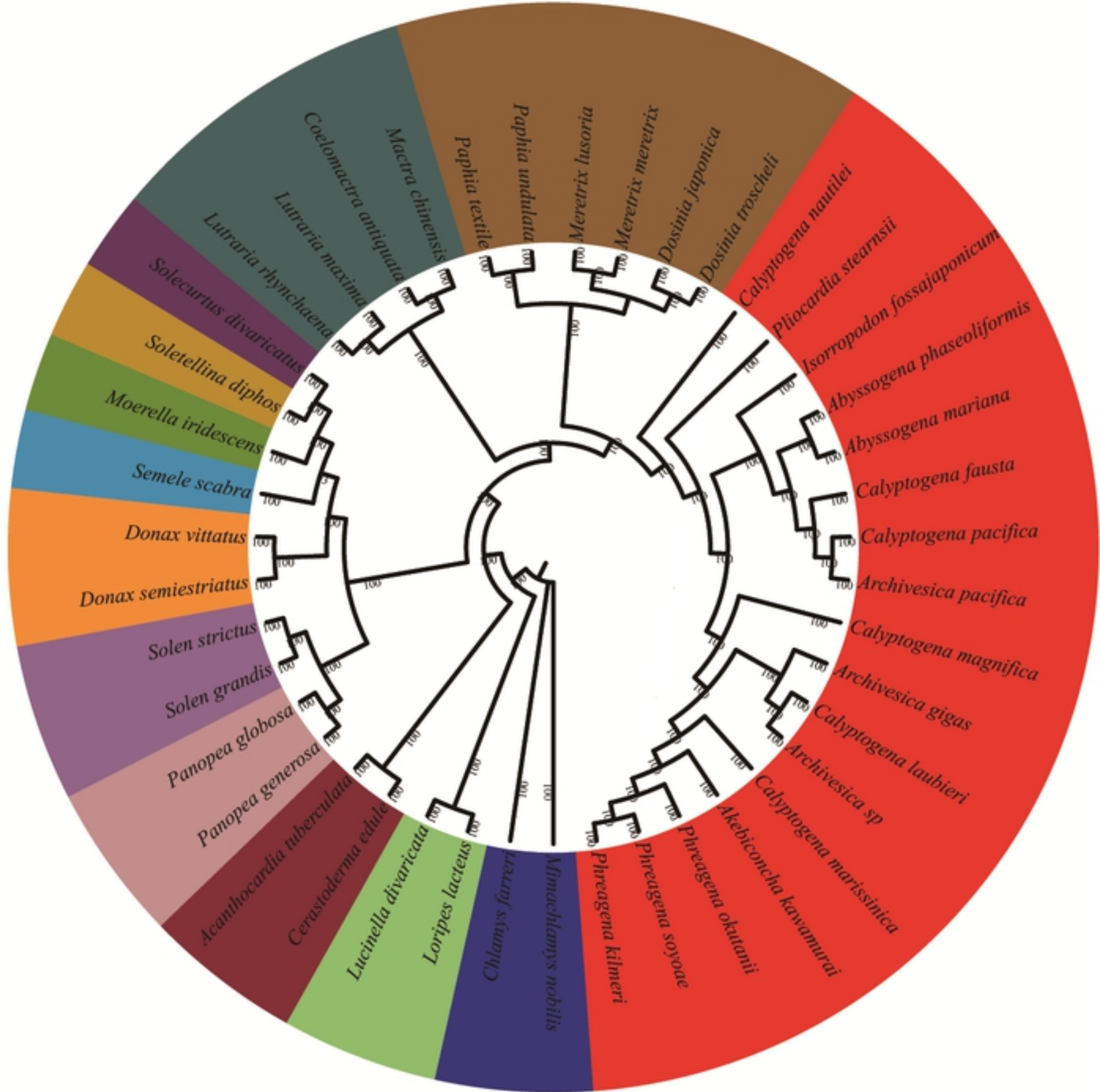


Figure 5